TERA

UNITED STATES OF AMERICA
NUCLEAR REGULATORY COMMISSION

BEFORE THE ATOMIC SAFETY AND LICENSING BOARD

In the Matter of	)	
	)	Docket 50-344
PORTLAND GENERAL ELECTRIC COMPANY,	)	
et al	)	(Control Building Proceeding)
	)	
(Trojan Nuclear Plant)	)	

CERTIFICATE OF SERVICE

I hereby certify that on July 10, 1979, Licensee's letter to the Director of Nuclear Reactor Regulation dated July 10, 1979 and an attachment entitled "Request for Additional Information, Trojan Nuclear Plant, Proposed Control Building Design", have been served upon the persons listed below by depositing copies thereof in the United States mail with proper postage affixed for first class mail.

Marshall E. Miller, Esq., Chairman
Atomic Safety and Licensing Board
U. S. Nuclear Regulatory Commission
Washington, D. C. 20555

Dr. Kenneth A. McCollom, Dean
Division of Engineering,
Architecture and Technology
Oklahoma State University
Stillwater, Oklahoma 74074

Dr. Hugh C. Paxton
1229 - 41st Street
Los Alamos, New Mexico 87544

Atomic Safety and Licensing Board
Panel
U. S. Nuclear Regulatory Commission
Washington, D. C. 20555

Atomic Safety and Licensing Appeal
Panel
U. S. Nuclear Regulatory Commission
Washington, D. C. 20555

Docketing and Service Section
Office of the Secretary
U. S. Nuclear Regulatory Commission
Washington, D. C. 20555

Joseph R. Gray, Esq.
Counsel for NRC Staff
U. S. Nuclear Regulatory Commission
Washington, D. C. 20555

Lowenstein, Newman, Reis, Axelrad &
Toll
1025 Connecticut Avenue, N. W.
Suite 1214
Washington, D. C. 20036

Richard M. Sandvik, Esq.
Assistant Attorney General
State of Oregon
Department of Justice
500 Pacific Building
520 S. W. Yamhill
Portland, Oregon 97204

William Kinsey, Esq.
Bonneville Power Administration
P. O. Box 3621
Portland, Oregon 97208

586054 7908080020

G

CERTIFICATE OF SERVICE

Ms. Nina Bell
728 S. E. 26th Avenue
Portland, Oregon 97214

Mr. John A. Kullberg
Route 1, Box 250Q
Sauvie Island, Oregon 97231

Mr. David B. McCoy
348 Hussey Lane
Grants Pass, Oregon 97526

Ms. C. Gail Parson
P. O. Box 2992
Kodiak, Alaska 99615

Mr. Eugene Rosolie
Coalition for Safe Power
215 S. E. 9th Avenue
Portland, Oregon 97214

Columbia County Courthouse
Law Library
Circuit Court Room
St. Helens, Oregon 97051

Dr. Harold Laursen
1520 N. W. 13th
Corvallis, Oregon 97330

G. A. Zimmerman

G. A. Zimmerman
Supervisor, Licensing Section
Generation Licensing & Analysis

Dated: July 10, 1979

586055

4sb66.27B8

PGE Portland General Electric Company

Donald J. Broehl Assistant Vice President

July 10, 1979

Trojan Nuclear Plant
Docket 50-344
License NPF-1

Director of Nuclear Reactor Regulation
ATTN: Mr. A. Schwencer, Chief
Operating Reactors Branch #1
Division of Operating Reactors
U.S. Nuclear Regulatory Commission
Washington, D. C. 20555

Dear Sir:

Enclosed are the answers prepared by Bechtel Power Corporation to the remaining five questions from your letter of May 18, 1979. This submittal answers the last of the formal questions posed by your staff. A revision to PGE-1020 covering updated information will be issued shortly.

Sincerely,

Donald J. Broehl

c: Mr. R. H. Engelken
Nuclear Regulatory Commission

Mr. Lynn Frank
State of Oregon
Department of Energy

586056

Discuss in detail how the effects of creep and shrinkage (e.g. dead weight reductions, tension fields etc.) have been factored into your consideration of the walls' shear strengths and stiffnesses.

Answer:

Creep of concrete is the time-dependent deformation resulting from the presence of stress whereas shrinkage in concrete is its contraction due to drying and chemical changes dependent on time and on moisture conditions, but not on stresses. Generally both creep and shrinkage have little effect on the strength of the structure, but they will cause a redistribution of stress in reinforced concrete members at the service load deflections. In the Complex walls, however, the shear walls are interrupted at the floor levels by the structural steel beams which, due to long term creep and shrinkage deformations of the walls, may cause some redistribution of the direct dead load of the walls and transfer it to the encased structural steel columns. Normally, such a redistribution will not have any adverse effect on the overall structure as the steel columns have adequate reserve capacity to withstand the effect of additional load. However, since both the capacity and stiffness of the walls are dependent upon the level of dead load stress on them, a reduction in dead load, if any, would have some effect on their shear resistance capabilities.

Several empirical methods exist for the calculation of creep strains. The most widely used method is that recommended by ACI Committee 209. The method gives the creep coefficient of concrete C_t as a function of several dependent variables, where C_t is the ratio of creep strain to initial elastic strain. The calculated value of the total long-term unrestrained strain of a typical wall panel is considered in conjunction with the axial stiffness of the wall, the bending stiffness of the floor beam and the axial stiffness of the steel column. It is found that in order to maintain displacement compatibility in the area of the beam-column connection and the adjacent portion of the wall panel, approximately 5% of the direct wall load will be transferred to the steel column. This evaluation provides an upper bound estimate since it ignores the part of the dead load which is transferred directly through the outside continuous masonry wythe and considers the entire dead load as coming through the floor beam. The analysis also ignores the stress relieving effect of the local creep in the zones where the load is being transferred from the walls to the encased steel frame. The local creep will tend to relieve the stress buildup in the concrete adjacent to the beam-column connection which will in turn reduce the load transferred from the walls to the steel frame due to the overall creep and shrinkage.

Evaluation of shrinkage strain in the walls of the Complex is difficult to quantify. It is generally accepted that moisture content and shrinkage strain are directly related, and therefore from the moisture diffusion phenomenon the migration of moisture through concrete as a function of time would provide an indication of the shrinkage strain if the boundary conditions and physical properties are properly specified. In the Complex walls, however, the core concrete was poured in between the previously constructed masonry wythes which were used as formwork. Therefore, moisture in the concrete would not have a free passage to diffuse to the surface thereby allowing the concrete to dry out and shrinkage strain to develop. Results of tests reported in the paper, "Effects of Normal and Extreme Environment on Reinforced Concrete Structures" by Bresler and Iding, published in ACI SP 55-11, indicate that for specimens having thicknesses comparable to the thicknesses of the Complex walls, an unrestrained concrete shrinkage strain would be approximately 100 x 10^{-6} inch/inch. Since the wall panels in the Complex are constrained from free movement by at least the continuous reinforcing steel in the masonry wythes and because of the restriction in the passage of moisture flow, the resulting shrinkage strain will be considerably less than the above unrestrained value of 100 x 10^{-6} inch/inch. Based on the above, an appropriate value of shrinkage strain will be approximately 70 x 10^{-6} inch/inch, which would result in about a 5% shift of dead load from the wall to the steel column.

The long-term effect of creep and shrinkage in the existing walls of the Complex, therefore, will result in shifting of approximately 10% of the direct dead load from the wall to

POOR ORIGINAL

586059

the structural columns. This reduction in wall dead load has been accounted for in the percentage variation while considering wall stiffnesses, as explained in response to Question No. 47. For evaluation of the wall capacities in accordance with the procedure described in Section 3.4.2.2 of PGE-1020, the direct dead load has not been reduced. However, as explained in response to Question No. 14, the lateral loads on the Complex walls will cause a portion of the vertical column load to shift back to the walls, which for the OBE event has been neglected. Although the actual amount of the load shift is difficult to quantify, it is reasonable to assume that the effects of lateral load and creep and shrinkage in the composite walls will tend to compensate each other. Also, the response to Question No. 15 discusses that although the calculated maximum vertical amplification is 16%, a value of 30% has been assumed, resulting in a 13% dead load reduction. All the direct dead load at all levels of the walls has been reduced by this amount resulting in a conservative estimate of the wall dead load. Furthermore, as discussed in response to Question No. 43, the wall capacities have been conservatively evaluated in PGE-1020, and a realistic assessment, even with reduced direct dead load that could be caused by the effects of creep and shrinkage, will result in wall capacities much in excess to those reported in PGE-1020.

Q. 20. Page 1 of 2 pages

Provide the upper limits for the relative displacement of the Turbine and Control Buildings, considering the test results, in the areas where the existing shake space is being reduced by the addition of the steel plate and verify that there is adequate clearance everywhere.

Answer:

The table below provides the upper limits for the relative displacements of the Turbine and Control Buildings in the areas where the existing gap is affected by the addition of the steel plate. These areas are at the Turbine Building's floors at elevations 93'0 and 69'0 for movement in the east-west (EW) direction. For movement in the north-south (NS) direction, Turbine Building column S41 has to be considered. Displacements are given for the SSE since it results in slightly larger values than the OBE. The Control Building displacements are based on shear wall stiffnesses obtained from the test data. The gap provided, shown for comparison, provides adequate clearance everywhere.

	Maximum EW Displacements (Inch) SSE .25g	
	EL 93'	EL 69'
Turbine Building (TB) @ 5% damping	0.9	0.15

POOR ORIGINAL

586061

Control Building (CB) @ 5% damping	0.046	0.031
ABS Combination TB & CB	0.946	0.181
Gap provided after modifications are made as discussed in Response to Question No. 36	2.0	2.5

	Maximum NS Displacements (Inch) SSE .25g
	EL 93'
Turbine Building (TB) @ 5% damping	1.25
Control Building (CB) @ 5% damping	0.086
ABS Combination TB&CB	1.336
Gap provided at plate	4.0

586062

Provide the relationships between stiffness and load degradation vs. the number of stress cycles at the stress levels to which the walls are loaded to substantiate that the structure will withstand several OBEs followed by an SSE. Indicate the number of full stress reversal cycles considered for each event and the number of OBEs considered for evaluation purposes and the basis for each choice.

Answer:

The test specimens were subjected to many phases of cyclic loading as explained in Section 1.4.2, Appendix A of PGE-1020. In general, each of the load-controlled phases in the elastic range had two complete cycles while each of the deformation controlled phases in the inelastic range had three complete cycles. As shown in Table 40-1, six specimens were tested under cyclic loadings at various stress levels. Five of the six specimens (except L2) were subjected to many load cycles in the elastic range at stress levels varying between 0.45 and 0.71 times the ultimate stress. The L2 specimen was cycled a number of times in the inelastic range by controlling the deformation to ±0.2".

586063

The cycling in the elastic range was discontinued whenever the specimen had stabilized, i.e., the successive cycles did not cause any new crack, extend the existing cracks or noticeably increase the deformation. Further cyclic loading on a stabilized specimen would not have altered its behavior. For example, Table 40-2 shows the stabilizing nature of specimen A5 under 11 cycles at a stress level of 0.67 times the ultimate stress. From the behavior of the test specimens, it can be concluded that Trojan type shear walls can withstand without undue deterioration a large number of seismic oscillations at a stress level near 0.6 times the ultimate stress or less.

It is difficult to determine the number of OBEs at a given site or the number of full stress cycles per OBE. The OBE is generally considered to be the largest earthquake that could occur at the site during the life of the plant. For seismic qualification of equipment (which has low damping), IEEE-344 suggests 10 maximum stress cycles per OBE. The NRC Standard Review Plan also provides guidelines for the number of stress cycles for subsystem qualification which suggests the same number of cycles per OBE. For reinforced concrete structures which have higher damping, the number should be much smaller. The ability of a structure to withstand several OBEs depends on its capability to absorb energy as well as the strength of its major elements. The area under the hysteresis loops shown in Appendix A, PGE1020 indicates that the wall specimens develop much higher damping or energy absorbing capability than is considered in calculating the seismic design forces for the Complex. This higher damping capability and the results in Tables 40-1 and 40-2 provide good assurance that the Complex can adequately withstand several OBEs followed by an SSE.

The above discussion is based on a conservative assessment of the structural response. If a more realistic approach were taken, the following additional conditions exist. As mentioned above, the test specimens intrinsically exhibit higher damping than was used for determining the seismic design forces. This will not only reduce the number of full stress cycles to less than 10, but will also provide a reduction in the shear load on the walls, thereby reducing the amount of degradation. As indicated in Table 40-1, the test specimens, except L2, were subjected to load-controlled cycles, i.e. the shear load was brought up to a constant level in each cycle and the deflection developed accordingly. In the actual walls, this uncontrolled deflection cannot take place since the walls are connected by floor slabs which act as diaphrams. If a portion of a wall becomes slightly overloaded during an OBE and the stiffness starts to degrade, the deflection will be controlled since it is connected to other portions of the wall and adjacent walls. This will result in some redistribution of loads, resulting in less stiffness degradation from that obtained from the test specimen. The comparison of the capacities and the shear forces in the Complex (Section 3.5 of PGE 1020) shows there is adequate capacity so that if localized yielding should occur, it would be on a local basis and a total wall at a given level will not yield.

Table 40-1 Specimens Subjected to Many Cyclic Loadings

Specimen	Stress Level	No. of Cycles	Degradation of Stiffness (Secant Modulus)	Degradation of Load
A4	0.45 V_u*	10	-8%	0**
A5	0.67 V_u	11	12%	0
B4	0.66 V_u	21	9%	0
C1	0.68 V_u	11	25%	0
L1	0.71 V_u	5	21%	0
L2***	±0.2"	6	27%	26%

Notes:
- * V_u is the ultimate shear stress
- ** Cycling in a load controlled phase
- *** Cycling in the inelastic post-ultimate stage by controlling the deformation to be within ± 0.2".

Q. 40. Page 6 of 6 pages

Table 40-2 Behavior of Specimen A5 at a Stress Level of $0.67V_u$

Cycle	Current Stiffness/ Stiffness at Cycle 1	Average Deflection (inches)
1	1.0	0.01235
2	0.97	0.01285
3	0.96	0.01300
4	0.95	0.01335
5	0.93	0.01340
6	0.92	0.01340
7	0.92	0.01340
8	0.91	0.01360
9	0.91	0.01360
10	0.90	0.01370
11	0.88	0.01400

Q. 44. Page 1 of 3 pages

Provide the relative displacement profiles between the complex and other structures, along with the allowable, at the computed OBE stress levels in the walls and the factored OBE stress levels in the walls considering the test data results.

Answer:

The two structures which interface with the Complex are the Turbine Building and the Containment. The relative displacements of the Turbine Building and the Complex corresponding to an SSE event and the existing gap between the two structures are given in response to Question No. 20. The table below provides the displacements of the Complex (at the intersection of column lines E and 60) and the Containment for OBE and SSE events. The displacements of the Complex are based upon stiffnesses of the shear walls as obtained from the test data and as described in Appendix B of PGE-1020.

Elevation	Building	Maximum Displacements (inch)			
		OBE: 0.15g, $\beta = 2\%$		SSE: 0.25g, $\beta = 5\%$	
		N-S	E-W	N-S	E-W
117'	Complex	.060	.049	.061	.050
	Containment	.088	.088	.094	.094
93'	Complex	.032	.029	.033	.030
	Containment	.058	.058	.062	.062
77'	Complex	.024	.025	.024	.026
	Containment	.039	.039	.042	.042
65'	Complex	.017	.011	.017	.011
	Containment	.026	.026	.028	.028

The relative displacements of the two structures can be conservatively obtained by taking the absolute summation of the respective displacements at various levels. The gap provided exceeds the calculated relative displacements by a wide margin.

The deflections of the Complex due to a factored OBE condition were estimated as follows:

For each area of the R-wall, the unfactored OBE shear stress determined from the STARDYNE model was multiplied by 1.40. For this new shear stress value a new stiffness was estimated, using figures B9, B10, and B11 from PGE-1020. It was found that, for the worst area, the stiffness was reduced by a factor of 3.1 with the average stiffness reduction for the elements of the existing wall being about 1.6. The new structural elements are expected to have a smaller stiffness reduction. However, if all the elements present had their stiffness reduction factor reduced by a factor of 3.1, the displacements would increase by a factor of 1.4(3.1) = 4.3. Because the R-wall is the most heavily stressed wall, the factor as calculated above can be taken as an upper bound for the deflection increase in the Complex due to a factored OBE.

Since the Containment is constructed of prestressed concrete, it would be expected to maintain its stiffness to higher stress levels. This would cause the OBE factored loads to be associated with deflections 1.4 times those produced by the unfactored OBE loads. However, even if the Containment deflections were to double, the absolute sum of Containment and the Complex deflections will be less than the space provided.

The Control Building deflections at the Turbine Building interface for an SSE event are given in response to Question No. 20. The deflections for an OBE will be approximately 2% less than those for an SSE. If the OBE deflections are increased by a factor of 4.3 (as obtained above), a conservative estimate of the displacement corresponding to a factored OBE can be obtained. As can be seen from the response to Question No. 20, the computed displacements of the Complex for factored OBE, when combined absolutely with the Turbine Building displacements for an SSE, will result in combined relative displacements which are less than the gap provided.

Provide the secant modulus derived for each of the test specimens vs. stress level; a comparison of the experimental initial elastic modulus for the test specimens vs. that calculated using the formula in Section 2.2.1.3.2 of Appendix B; the error bands, and their deviation, for the curves representing stiffness reduction as a function of stress level; and the stresses in each of the walls resulting from incorporation of the stiffness reduction factors in the STARDYNE model along with the associated stiffness reduction factors assumed in the analysis.

Answer:

The secant modulus vs. shear stress for the test specimens is shown in Figures 46-1 through 46-20. A comparison between the experimental initial elastic modulus and that calculated using the formula in Section 2.2.1.3.2 of PGE-1020, Appendix B cannot be made since the initial modulus cannot be determined experimentally. The instrumentation was not sufficiently sensitive to measure the small deflections required for the calculation. Deflections need to be measured reliably to the nearest .0002 inch at the early stages of deformation. During this stage, the test specimen and load frame is settling in, play in instrumentation is being taken up, etc. Care was taken to minimize these effects but all could not be completely eliminated since the movements being considered are between 1 and 10 times smaller than the thickness of this paper. Some difficulty was even encountered at the first load step but for the other load steps the deflections were large enough so that effects were not important. As shown in Figures 46-1 to 46-20, there are in general two data points at the first load step. The top part is obtained from the average deflections recorded on each side of the specimen and the other is obtained from the most active dial gauge. The initial modulus used in the plot was calculated using the equation in PGE-1020, Appendix B. An error analysis of the data could not be made since there are not enough specimens with duplicate conditions to provide sufficient data base. The effect of variation is considered in the broadening of the response spectra.

Since the stiffness reduction factors are not linear with stress level discuss the effect of transverse gross overturning moments and transverse inertial wall loadings, plus the effects of creep and shrinkage on the stiffness in a given direction. Discuss the affects of the embedded steel framing and how it was incorporated into your analyses.

Answer:

It is well recognized that the stiffness of reinforced concrete structures reduces when the load is increased. For a shear wall system in general, this reduction is due to minor flexural cracking in the early stages of deformation and diagonal cracking in the final stages at deformation. The amount of stiffness reduction depends on the reinforcing steel ratio, and the magnitude of the lateral load and the axial load. In order to develop a rational approach to account for this reduction in stiffness, the stiffness of the test specimens was determined as a function of shear stress, reinforcing steel ratio and axial load. The results indictated the same general trends that have been observed by others. The stiffness reduction factor has been nondimensionalized to increase its applicability. The type of behavior experienced by the test specimens is generally the same type of behavior that the actual walls of the Complex will experience, i.e. bending deformation. The actual walls have the steel frame encased in them. In order to factor this into the stiffness determination, the presence of the frame has been considered as contributing to the overall bending moment resistance of the Complex and as such can be considered as additional reinforcing steel. The amount of reinforcing steel is related to the beam-column connection capacity and is taken as

$$A_s = \frac{4V}{\phi f_y D}$$

where V = AISC Table I allowable shear load for the beam-column connection

ϕ = capacity reduction factor, 0.9

f_y = yield stress of the reinforcing steel

D = depth of the panel for which the stiffness reduction factor is being determined

A_s = cross-sectional area of equivalent reinforcing steel per unit length.

The factor of 4 in the numerator results from the OBE capacity of the beam-column connection being twice the AISC Table I value; the other factor of two results from the shear being at the edge of the panel and therefore approximately twice as effective as uniformly distributed reinforcing steel.

In considering the variation of the stiffness due to gross bending moment, transverse inertia loads, creep and/or shrinkage, the significance of the variations should also be considered. The variation of stiffness due to shear stress is accounted for explicitly in the iteration process discussed in PGE-1020, Appendix B. The variations contributed from the other sources have been considered for their effects on the forces in the Complex walls and the floor response spectra. As is discussed in response to Question 47, the change in frequency due to the inclusion of the stiffness reduction factors is relatively small since the overall shear stresses are low. Since the change in frequency is small, the spectral acceleration associated with the various modes will only change slightly resulting in a small overall change in the inertia loads and associated forces in the Complex walls.

Possible variations in the stiffness could affect the floor response spectra by shifting the central frequency associated with the peaks. As indicated above, this change is small. Even though the stiffness reduction factor is a non-linear function of shear stress, the amount of shift cannot be significant and is accounted for in the broadening of the floor response spectra discussed in Question 47.

Q. 46. (c)

Also, indicate why the results of the specimens with struts were not incorporated into your stiffness considerations.

Answer:

The stiffness reduction factors are intended to be used to describe the stiffness of the composite sections of the Complex walls. To obtain this information from the specimens with the struts, the interaction of the steel struts, which are external, and the test specimen would have to be evaluated. This would be difficult and the results would necessarily depend on the simplifying assumptions.

If one assumes the struts were an extension of the test specimen resulting in an increase in reinforcing steel, a rough approximation might be obtained. Information in this reinforcing steel range, however, was obtained from specimens J1, L1 and L2 without making such assumptions.

Since the interaction between the specimen and the struts is difficult to evaluate with confidence and similar results are available from other specimens, stiffness results are not used from the specimens with struts.

586077

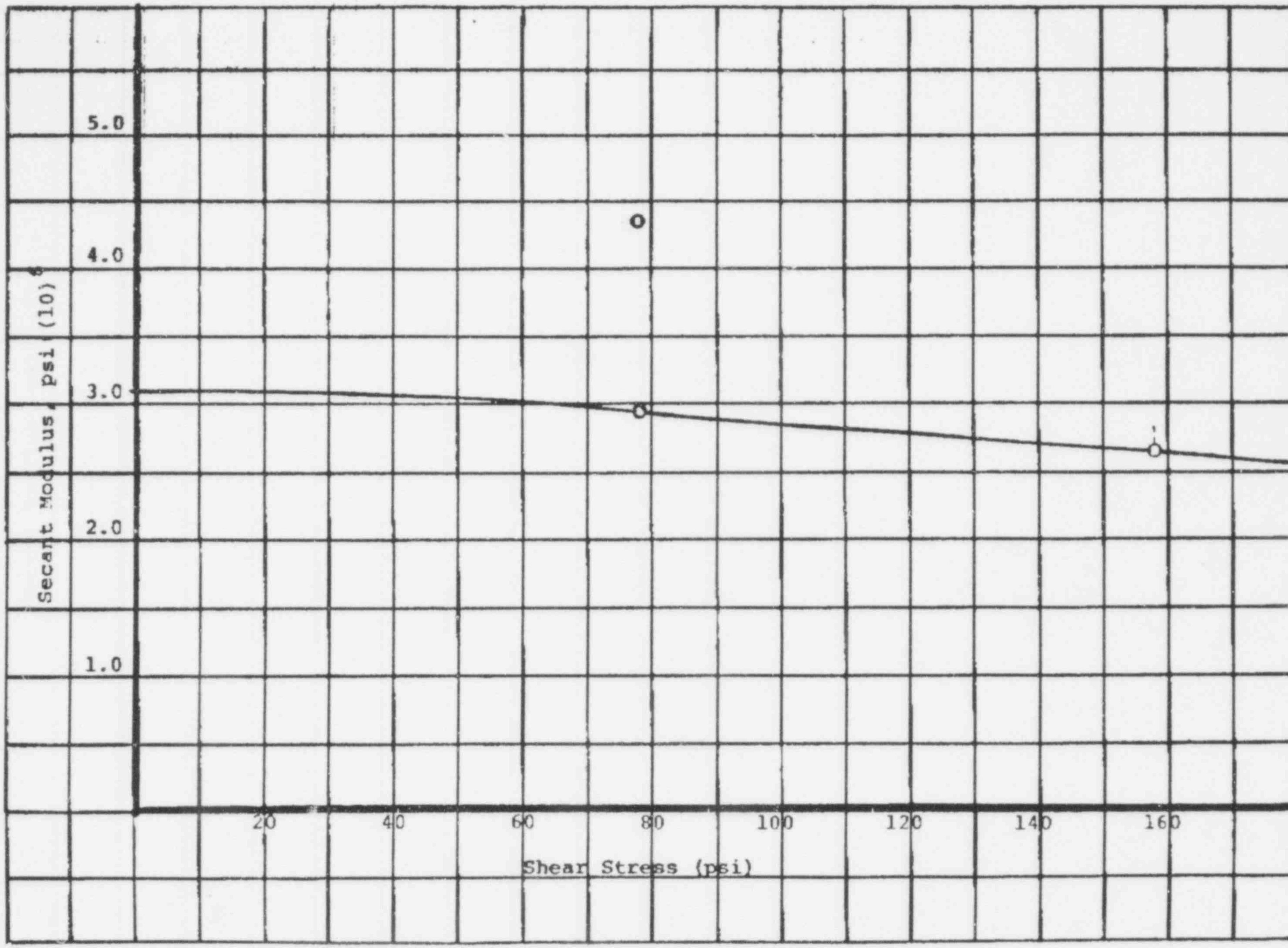

Figure 46-1 Secant Modulus, Specimen A-1

586078

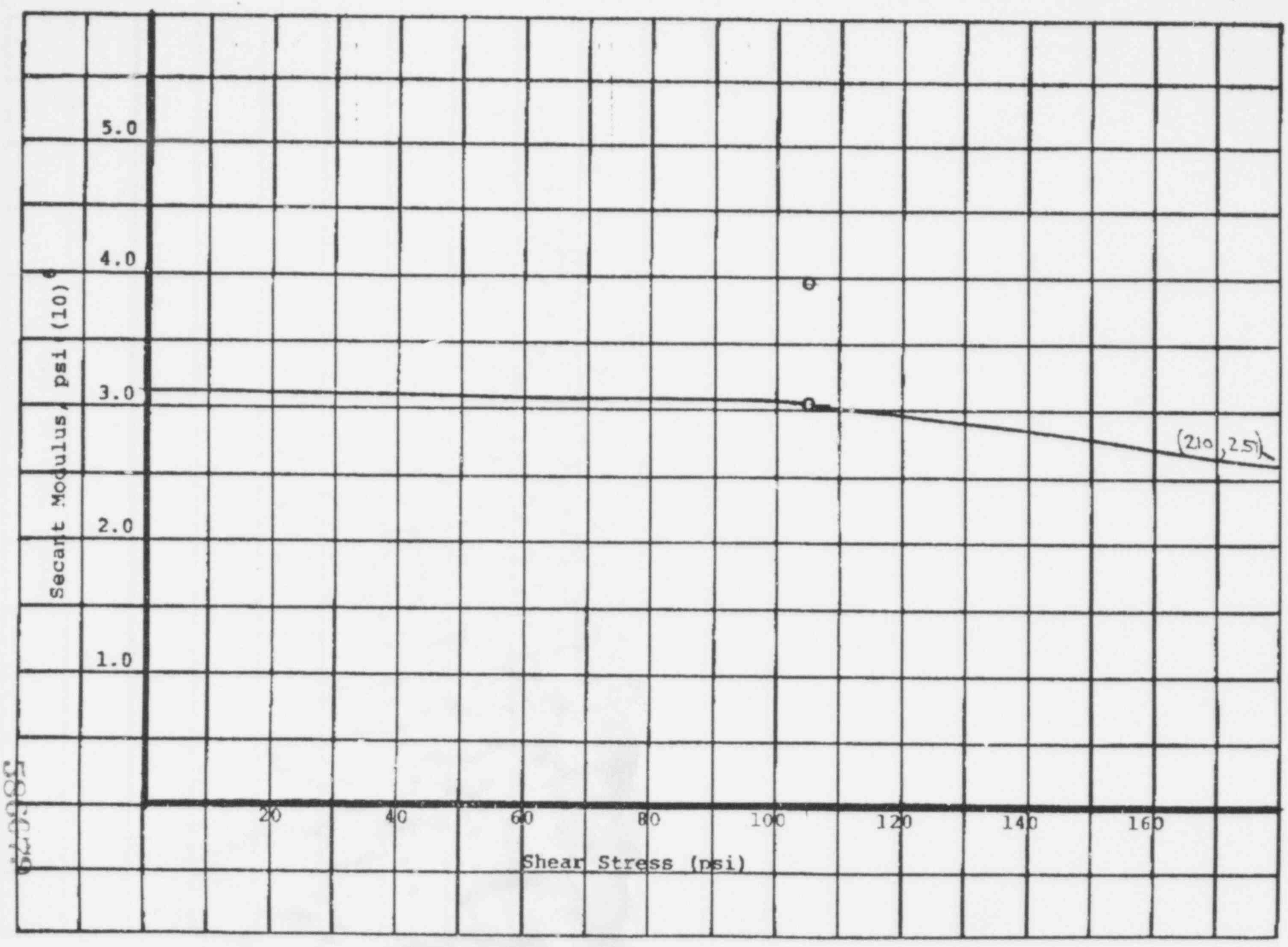

Figure 46- 2   Secant Modulus, Specimen A-2

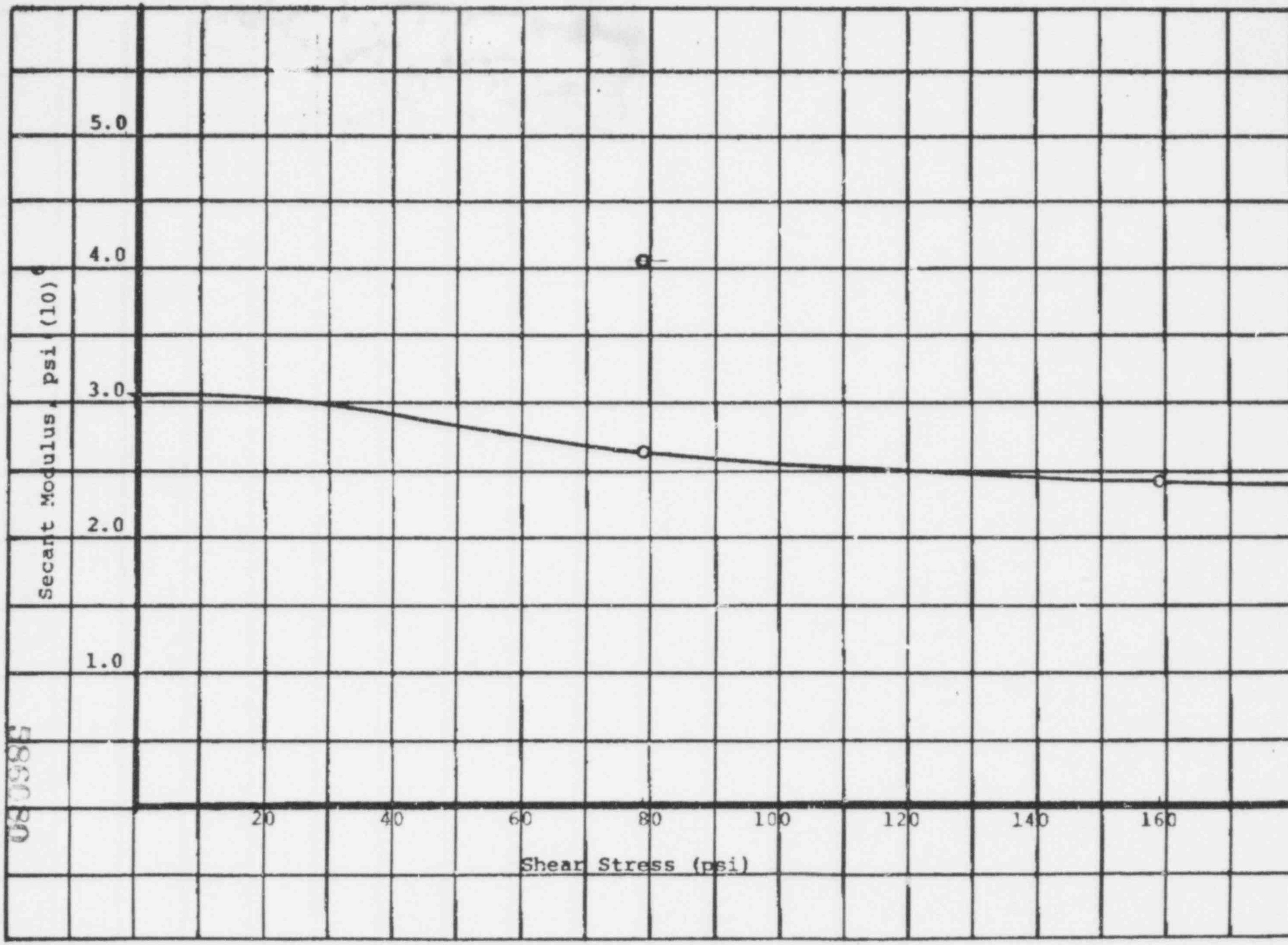

Figure 46- 3   Secant Modulus, Specimen A-3

586080

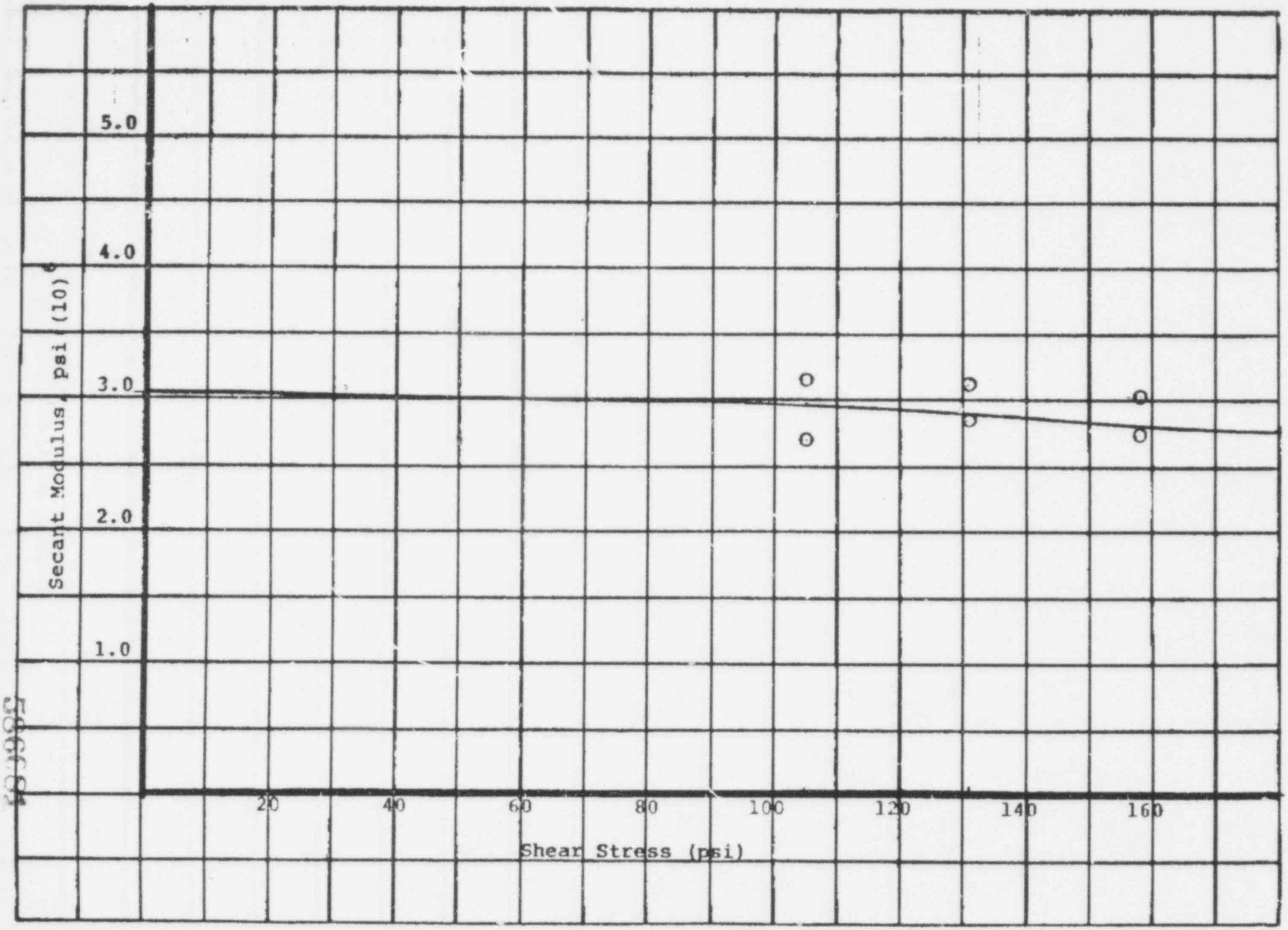

Figure 46- 4 Secant Modulus, Specimen A-4

586684

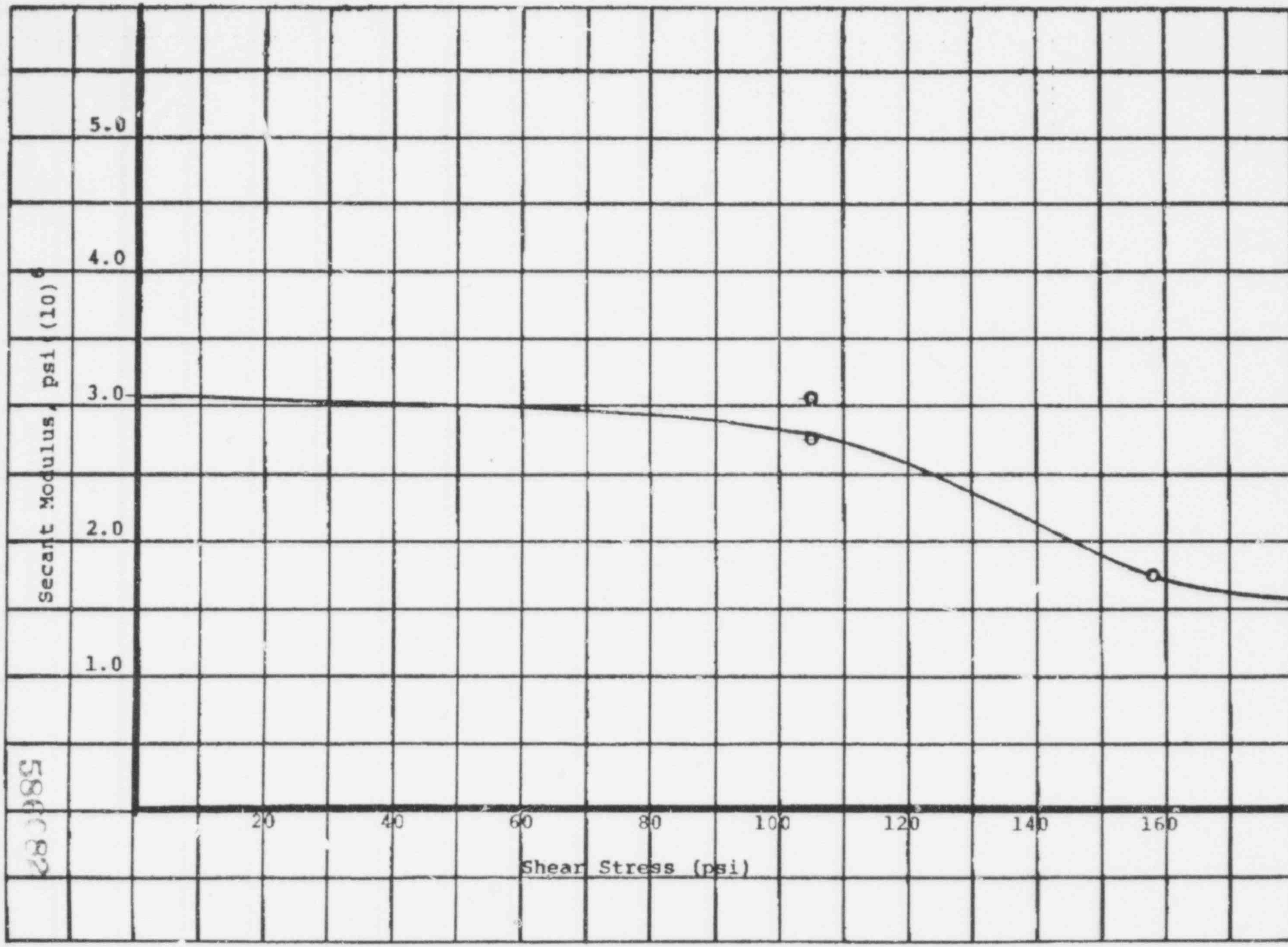

Figure 46-5 Secant Modulus, Specimen A-5

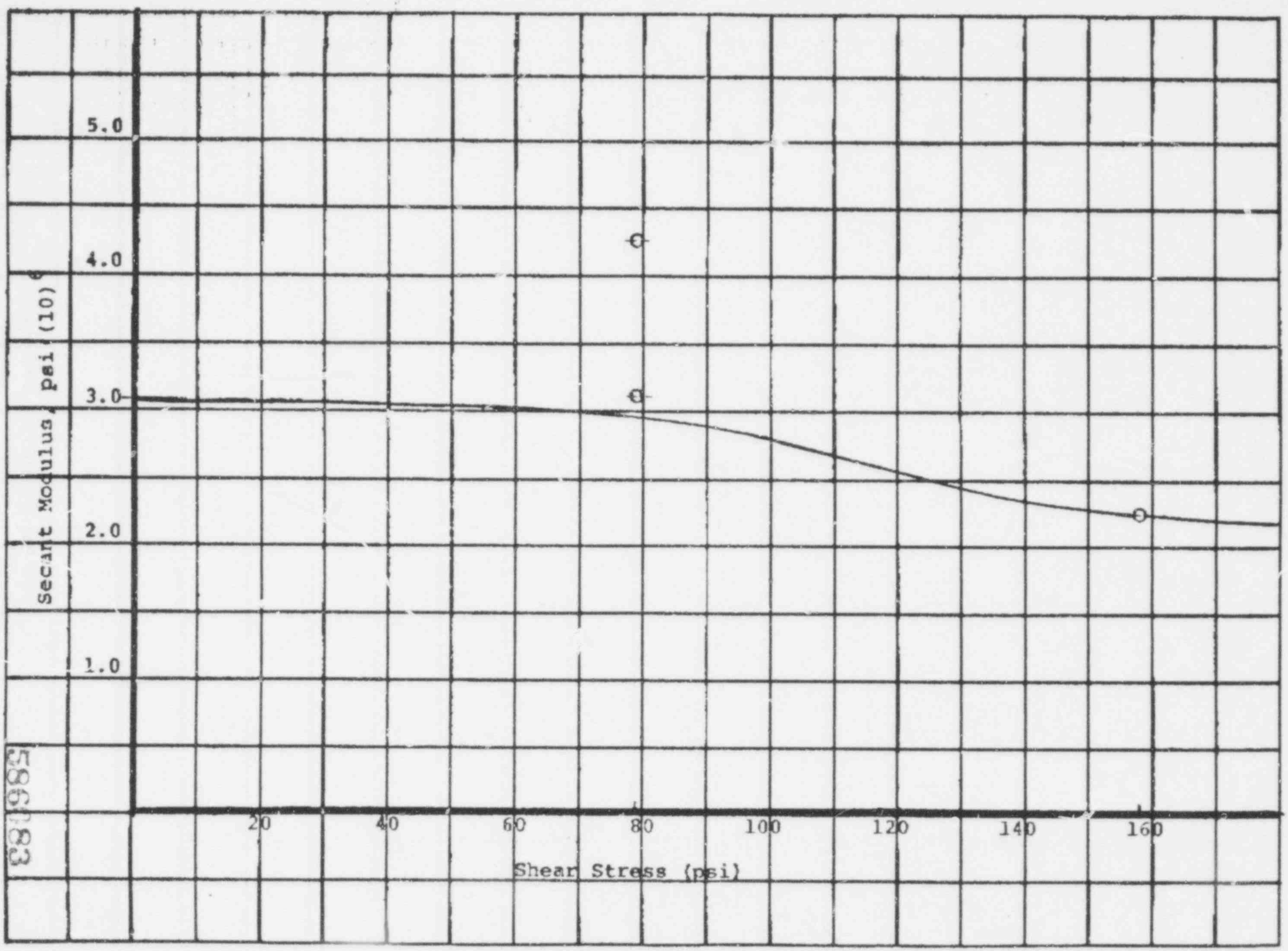

Figure 46-6   Secant Modulus, Specimen B-1

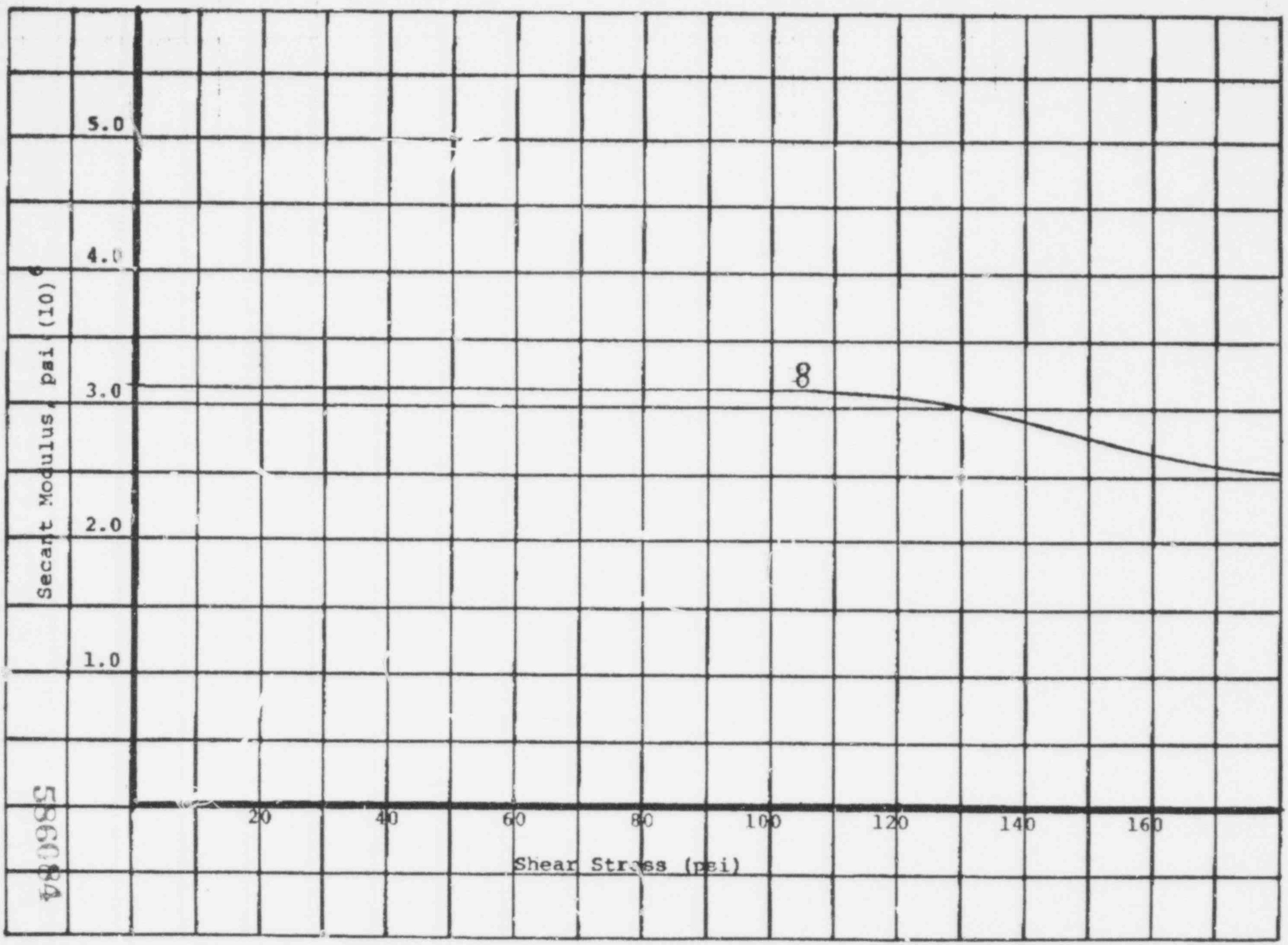

Figure 46-7 Secant Modulus, Specimen B-2

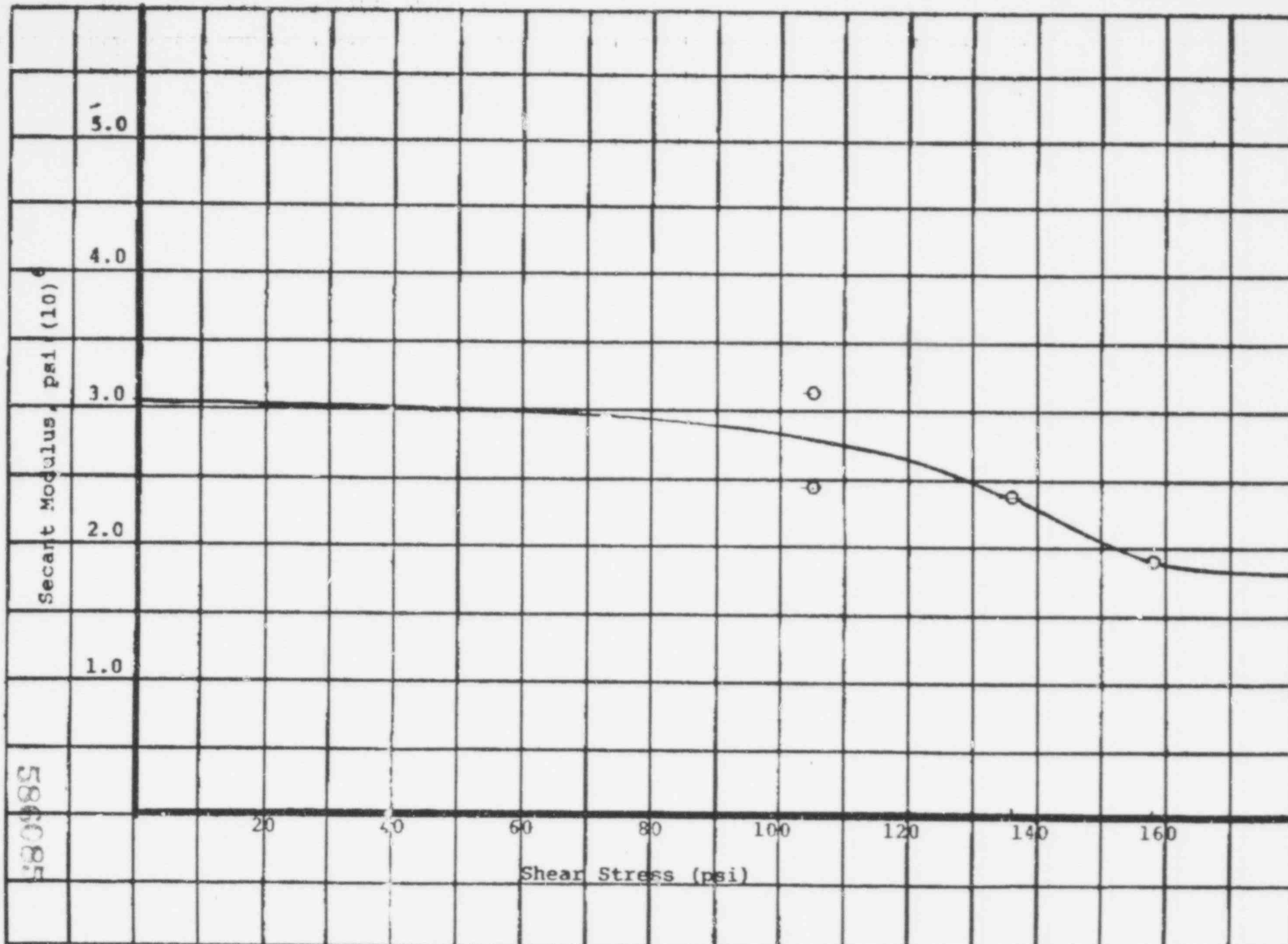

Figure 46-8 Secant Modulus, Specimen B-3

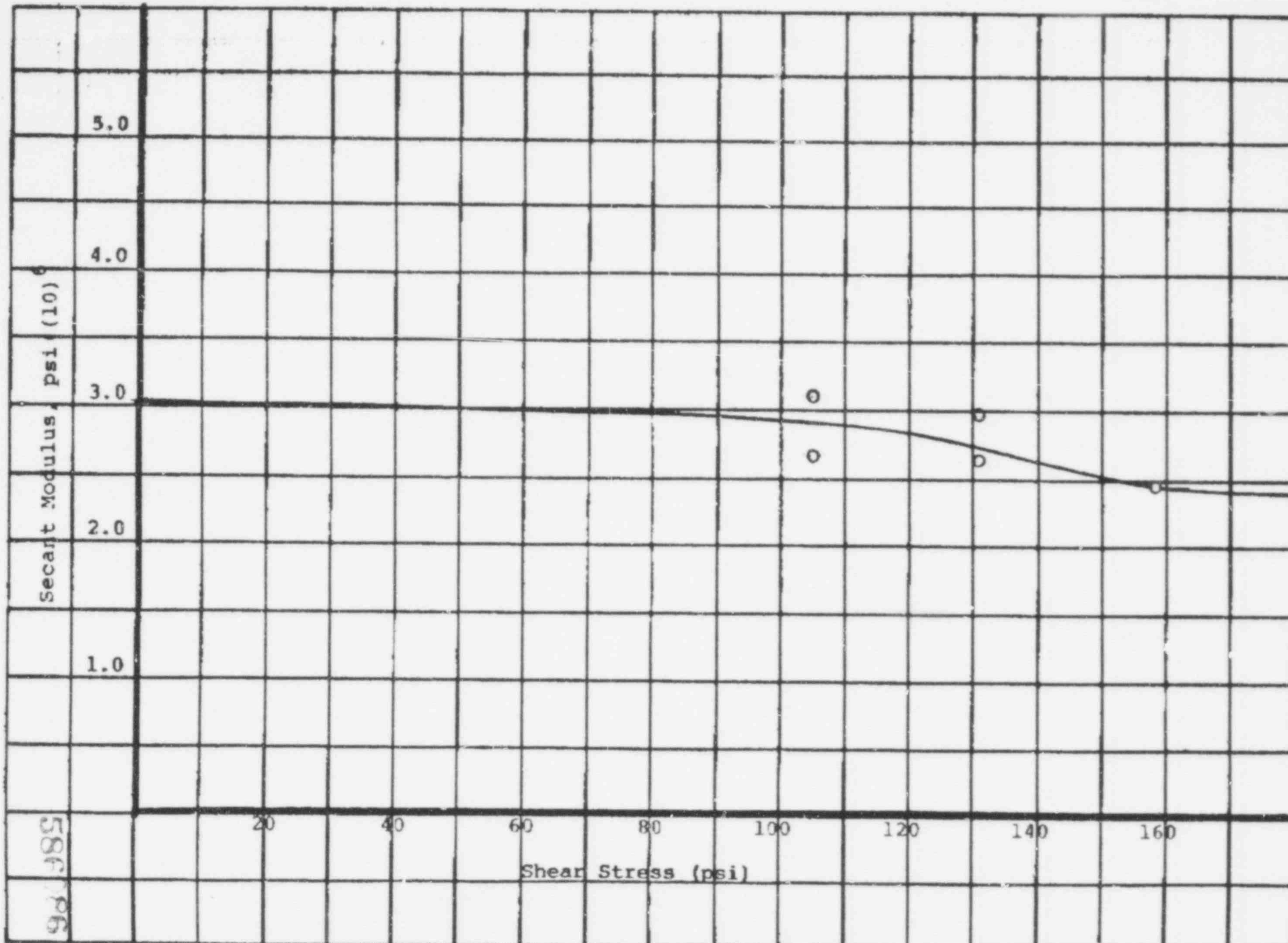

Figure 46-9 Secant Modulus, Specimen B-4

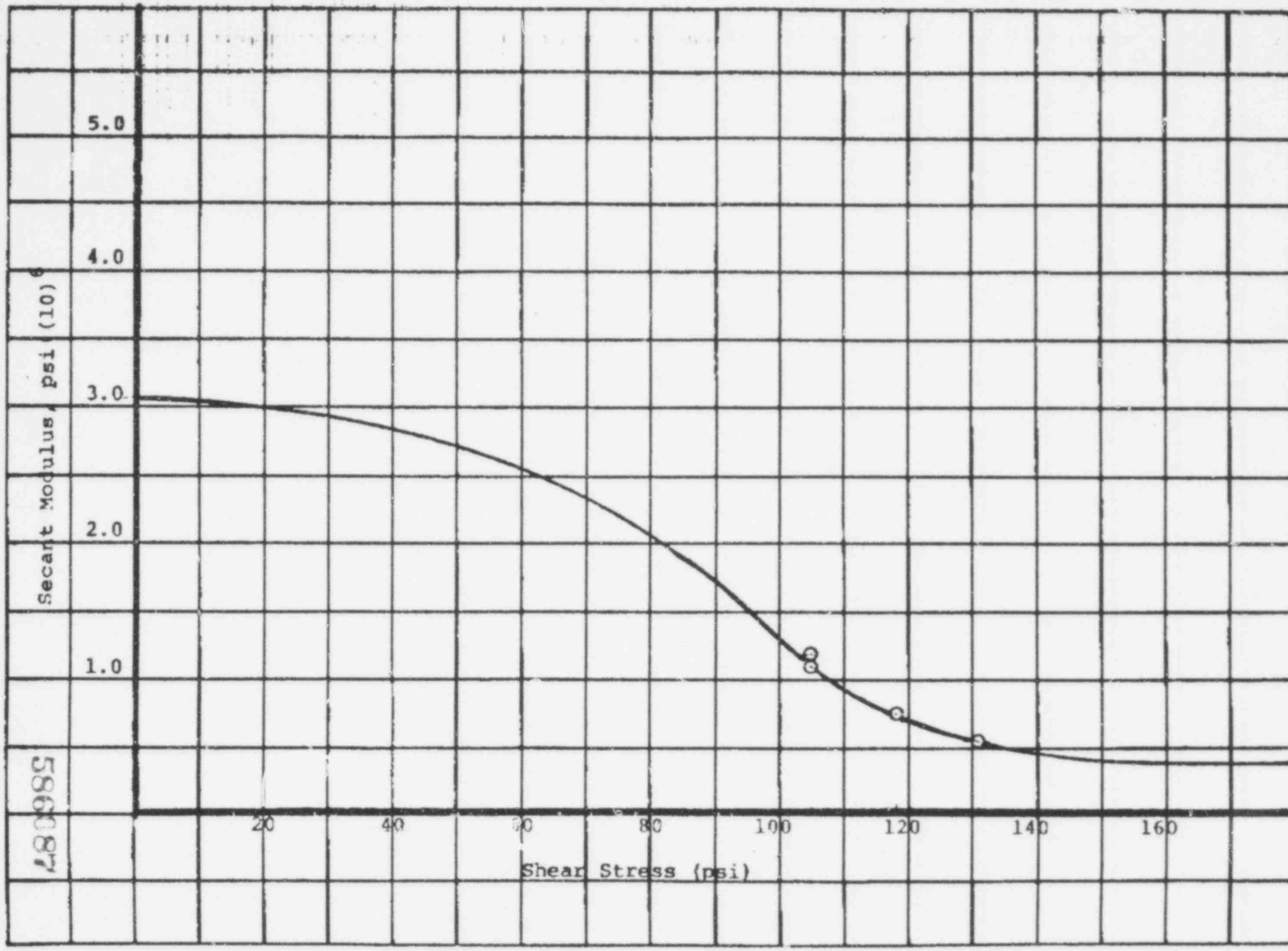

Figure 46- 10 Secant Modulus, Specimen B-5

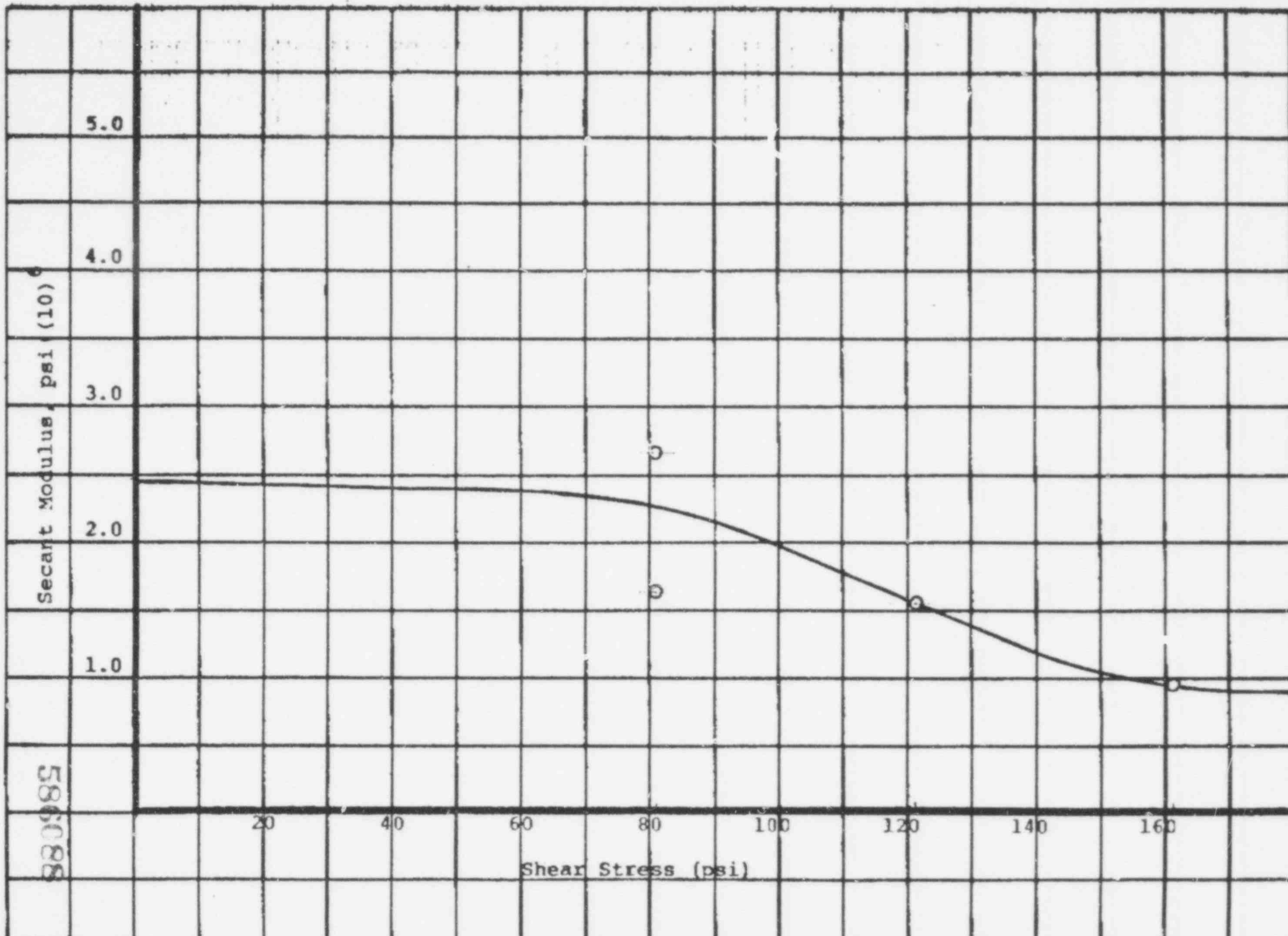

Figure 46-11 Secant Modulus, Specimen D-1

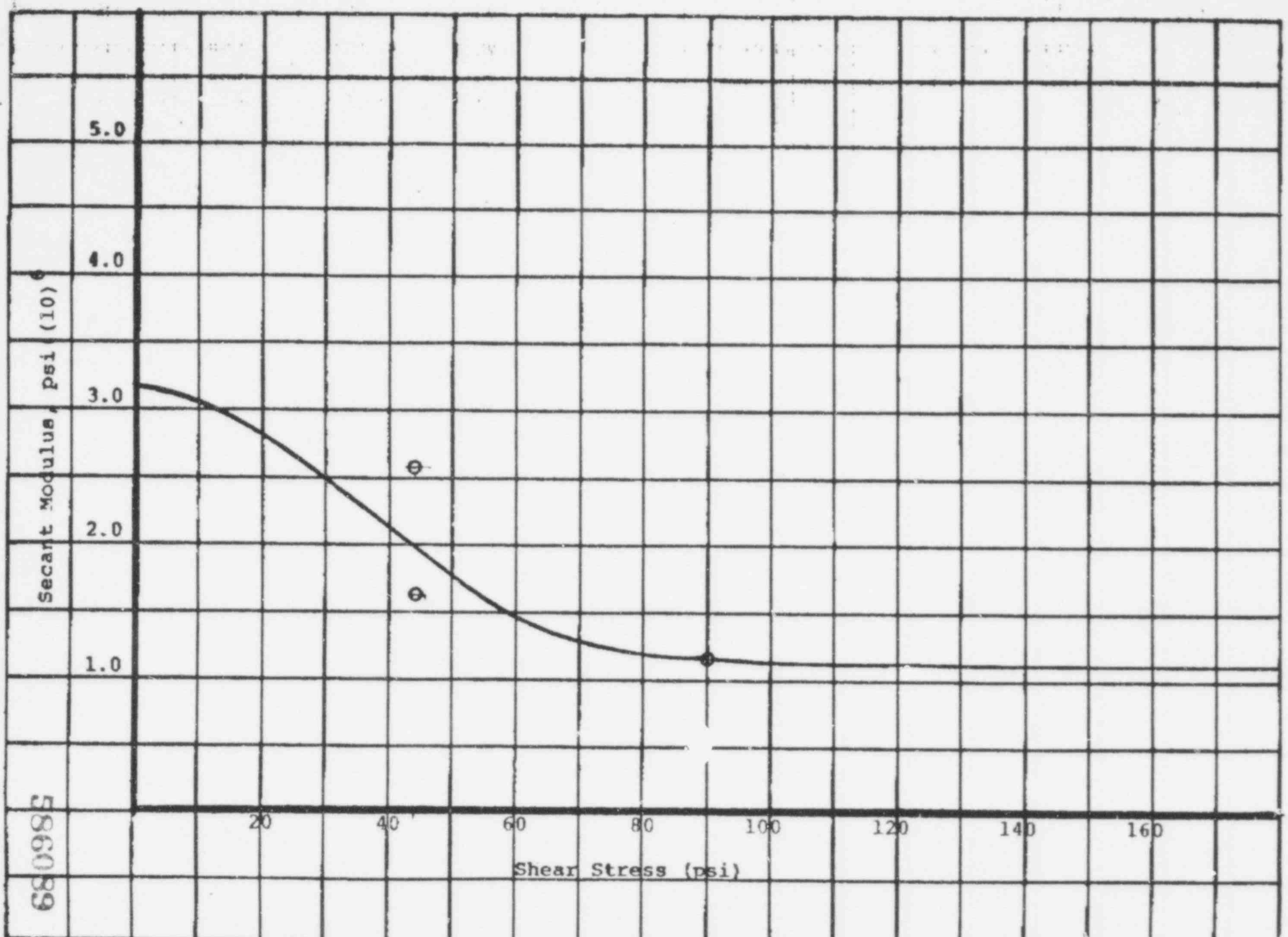

Figure 46-12 Secant Modulus, Specimen E-2

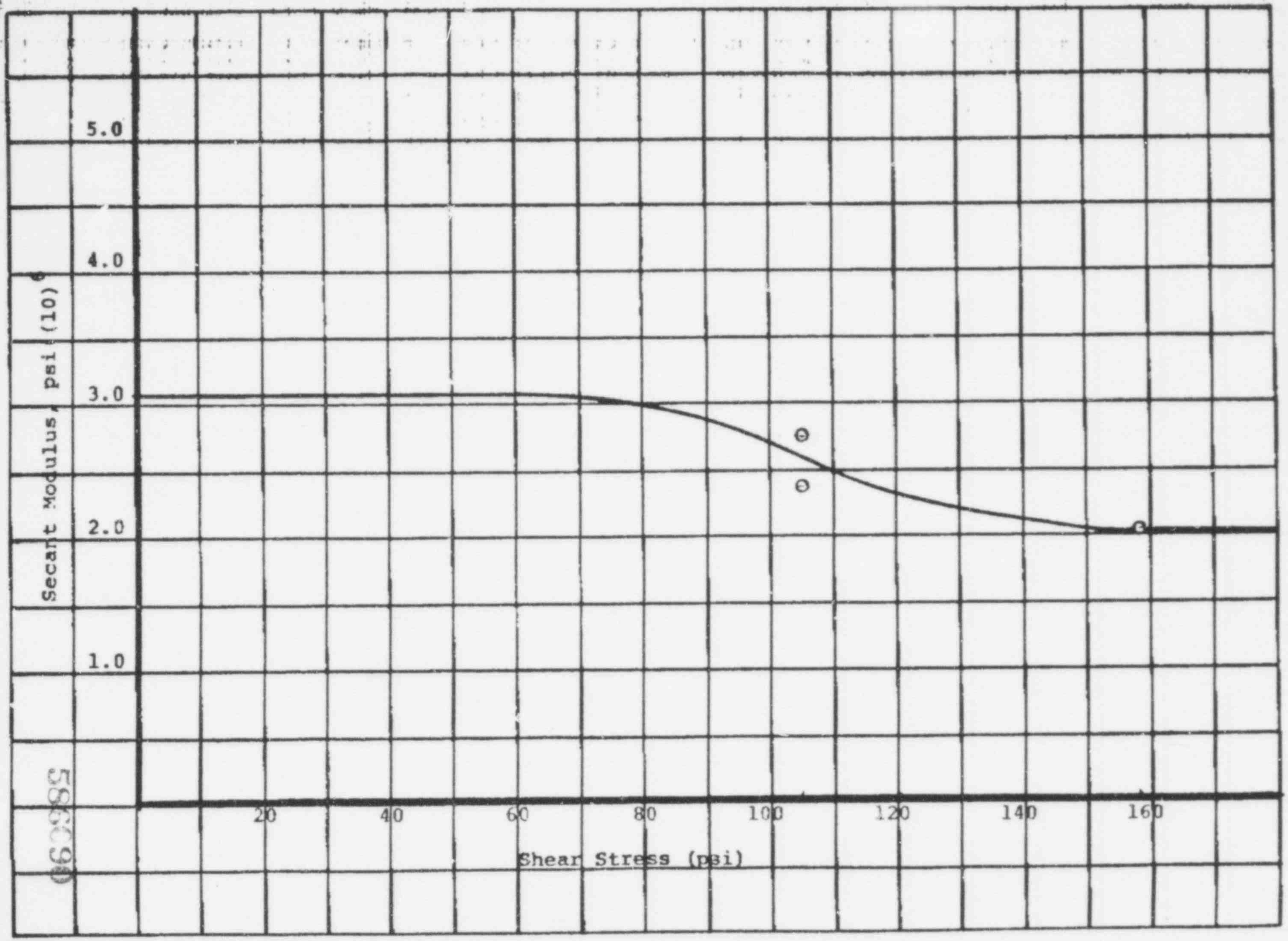

Figure 46- 13   Secant Modulus, Specimen   F-1

5866090

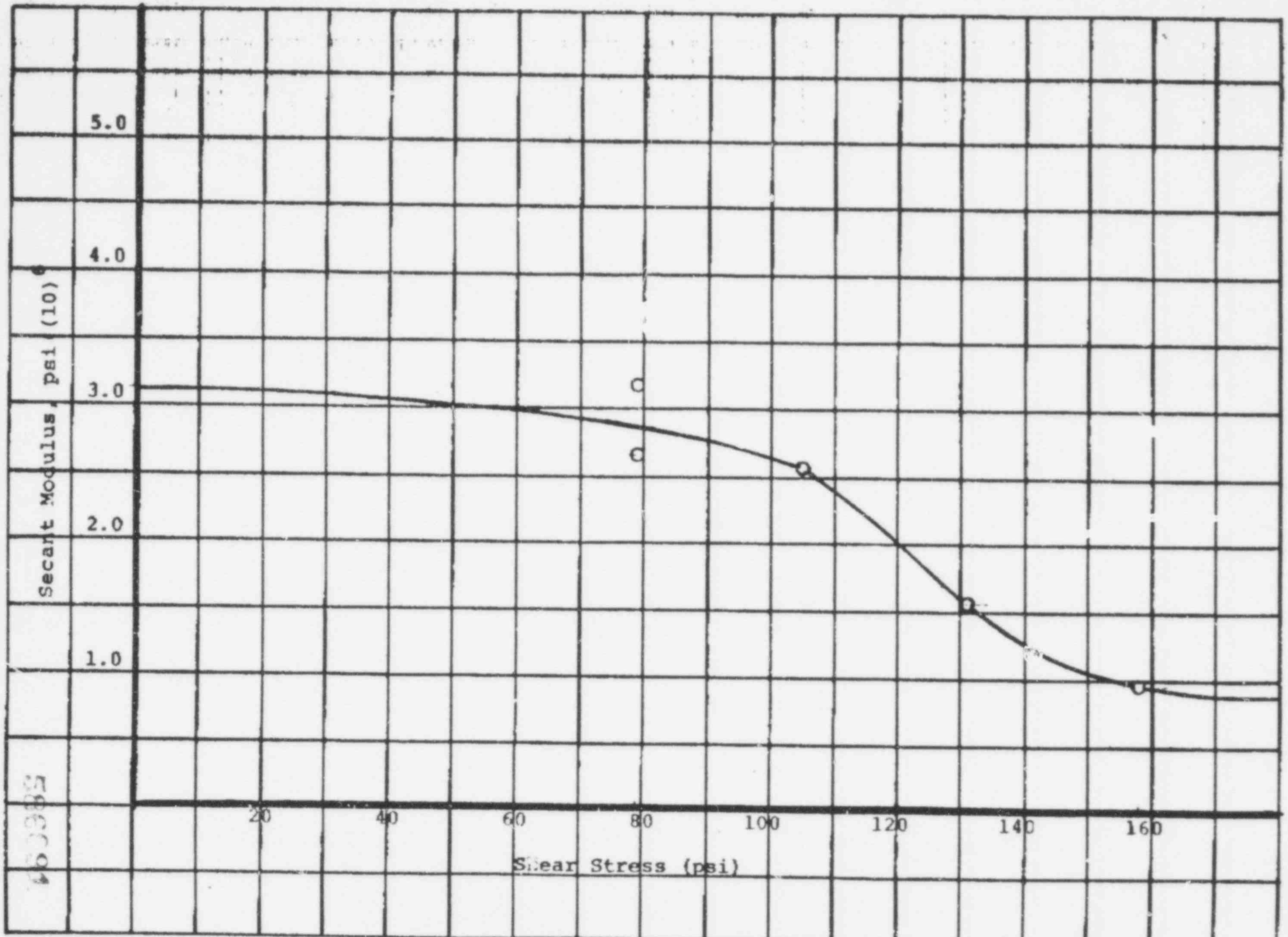

Figure 46-14 Secant Modulus, Specimen G-1

586084

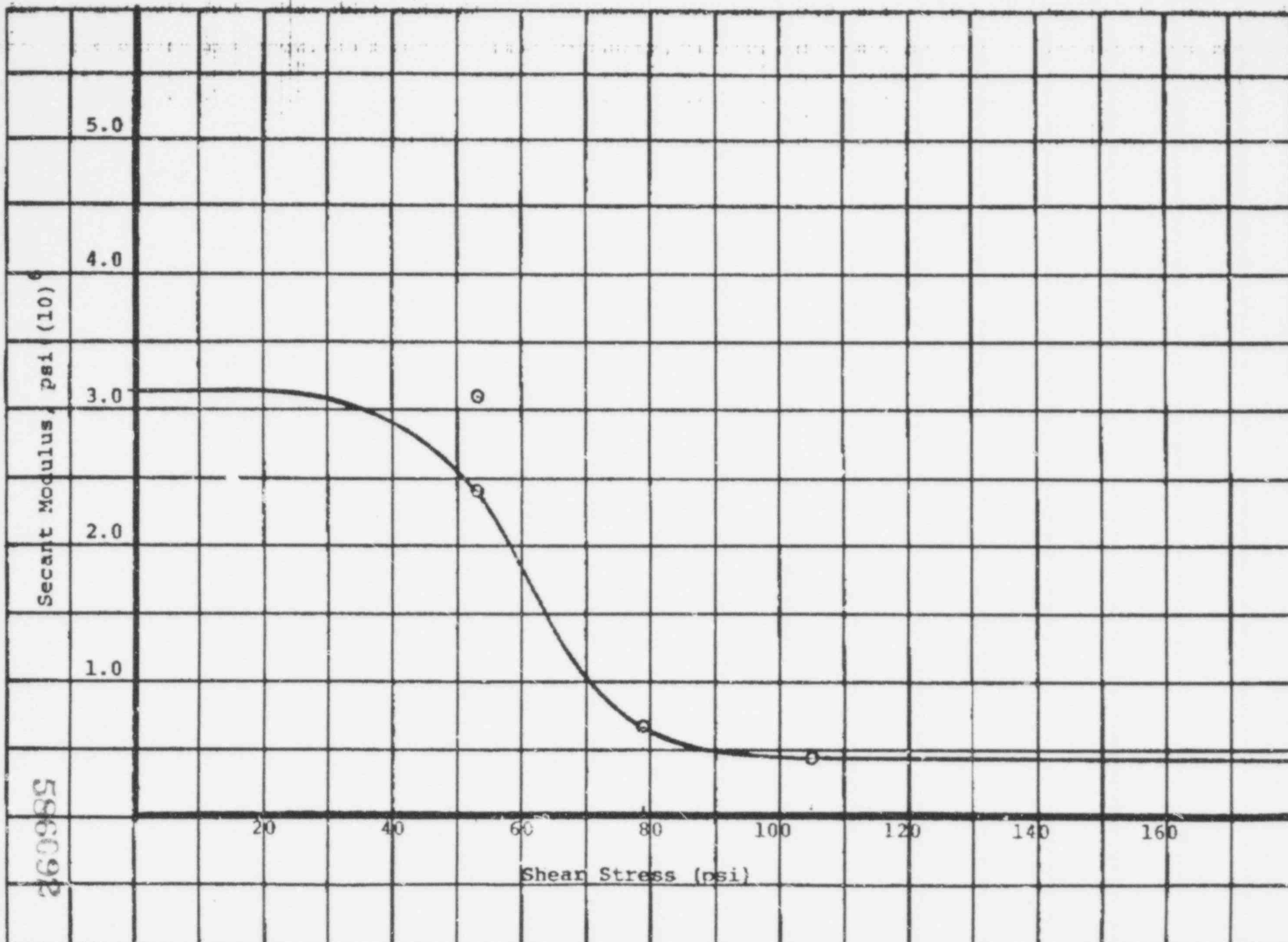

Figure 46-15 Secant Modulus, Specimen G-2

586092

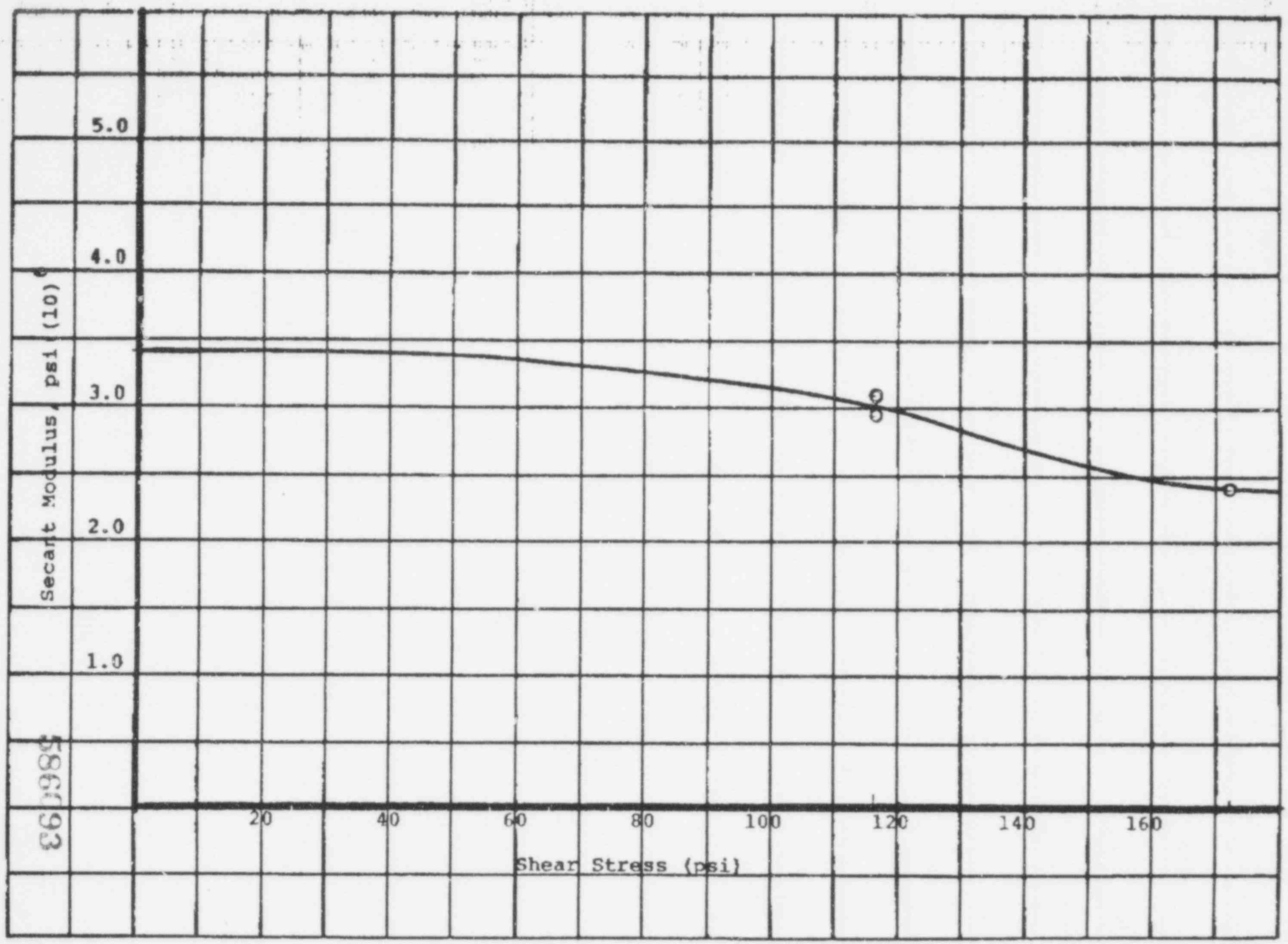

Figure 46-16 Secant Modulus, Specimen H-1

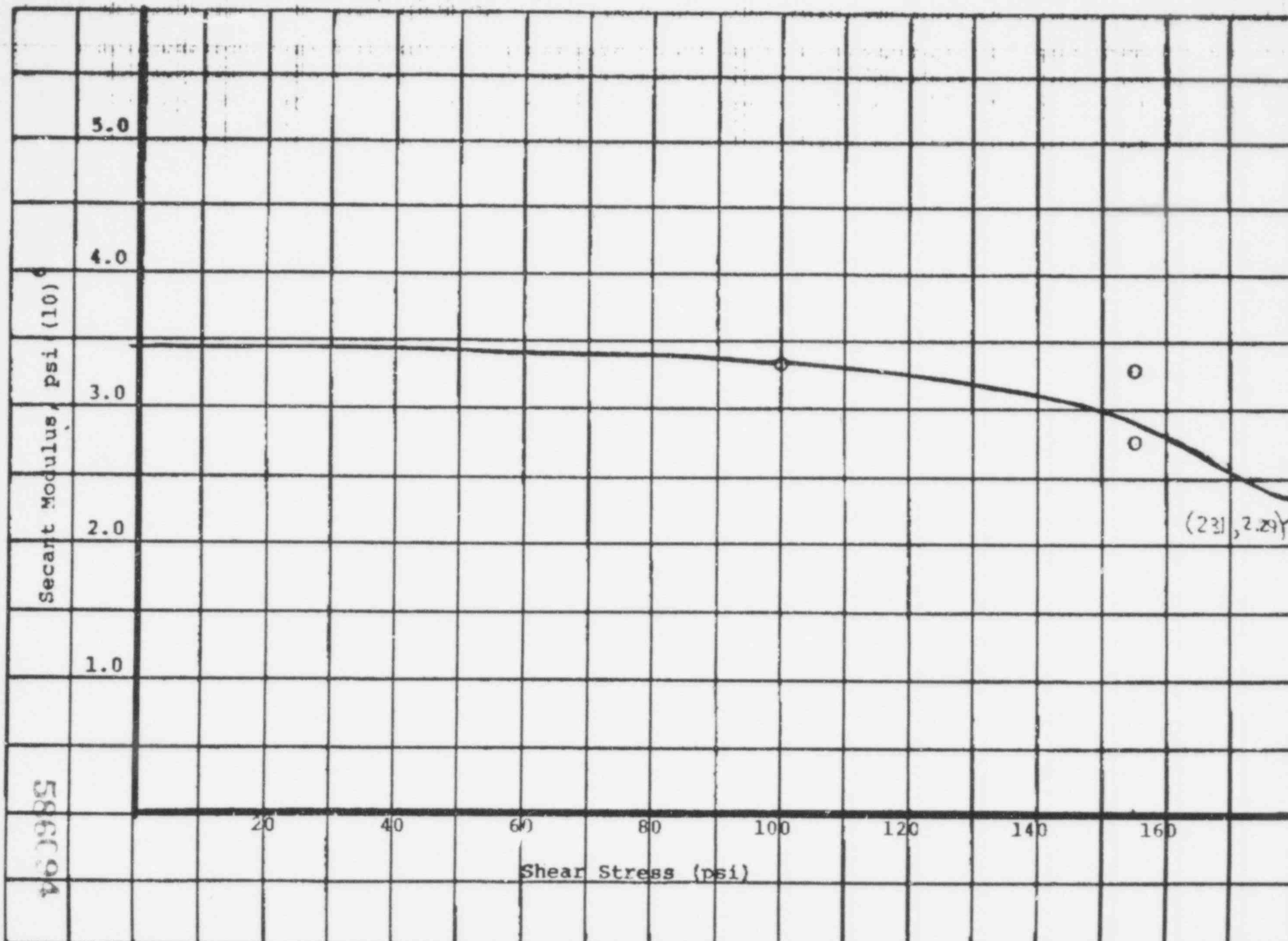

Figure 46-17 Secant Modulus, Specimen J-1

586094

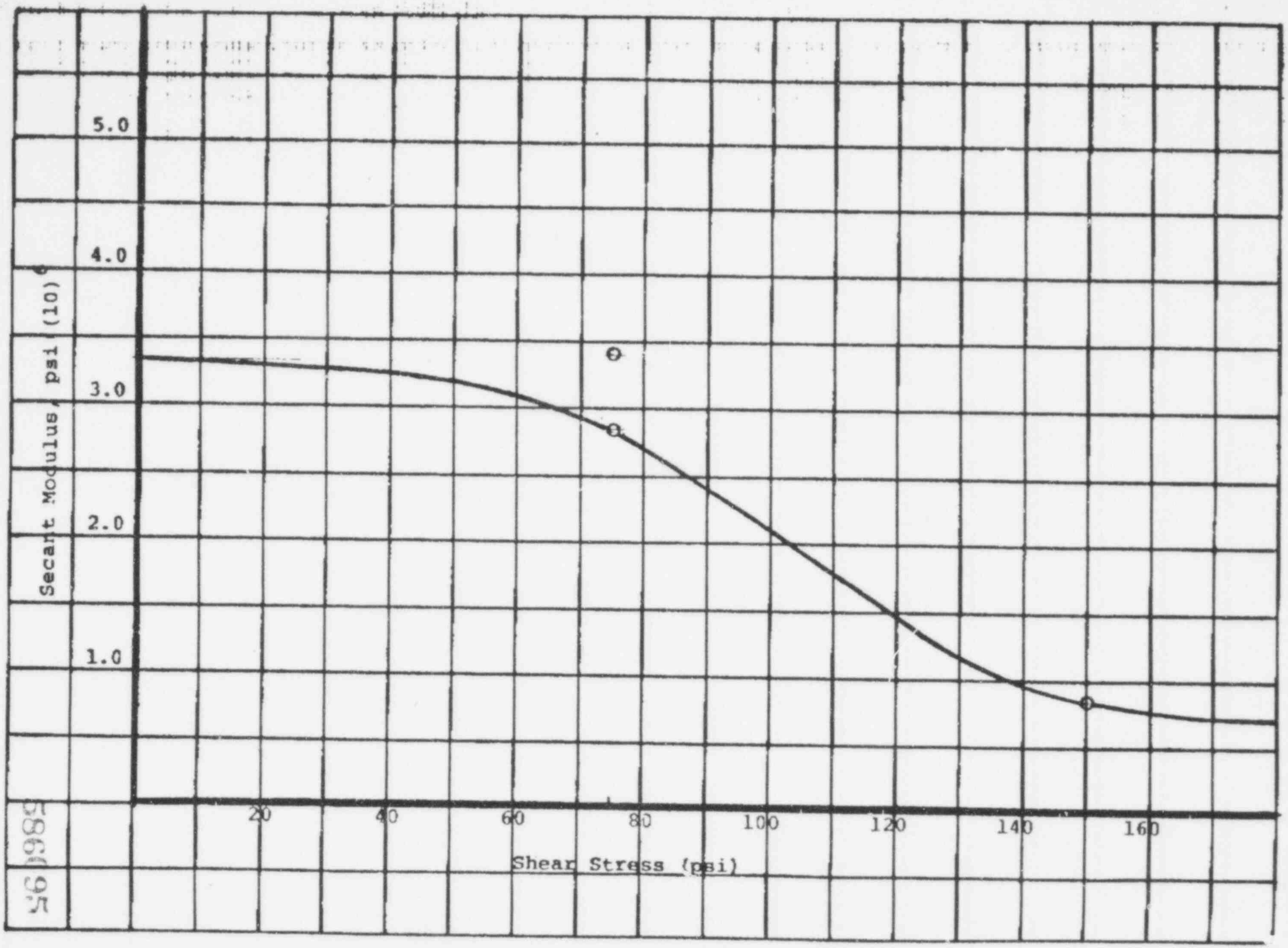

Figure 46-18 Secant Modulus, Specimen K-1

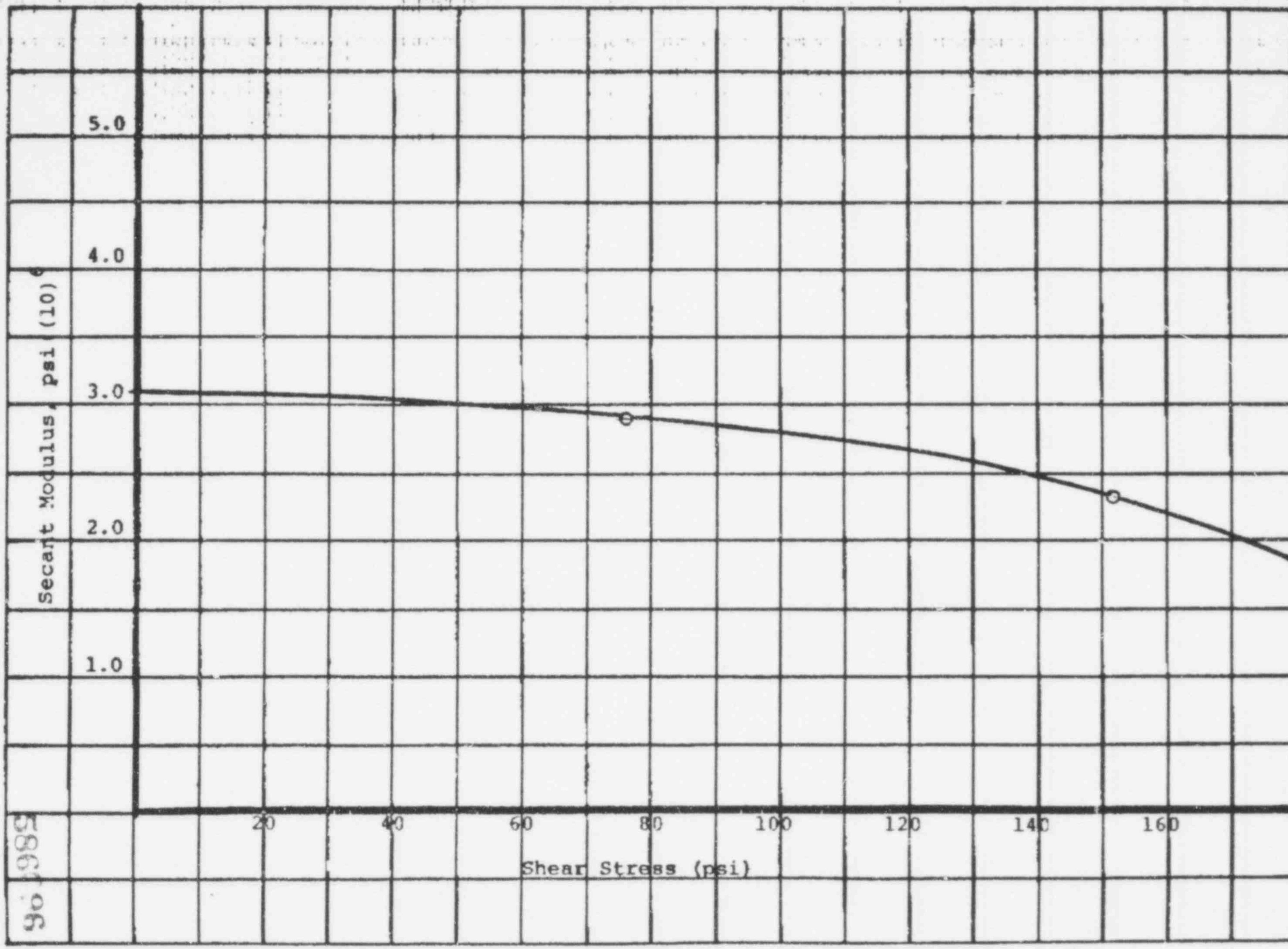

Figure 46- 19 Secant Modulus, Specimen L-1

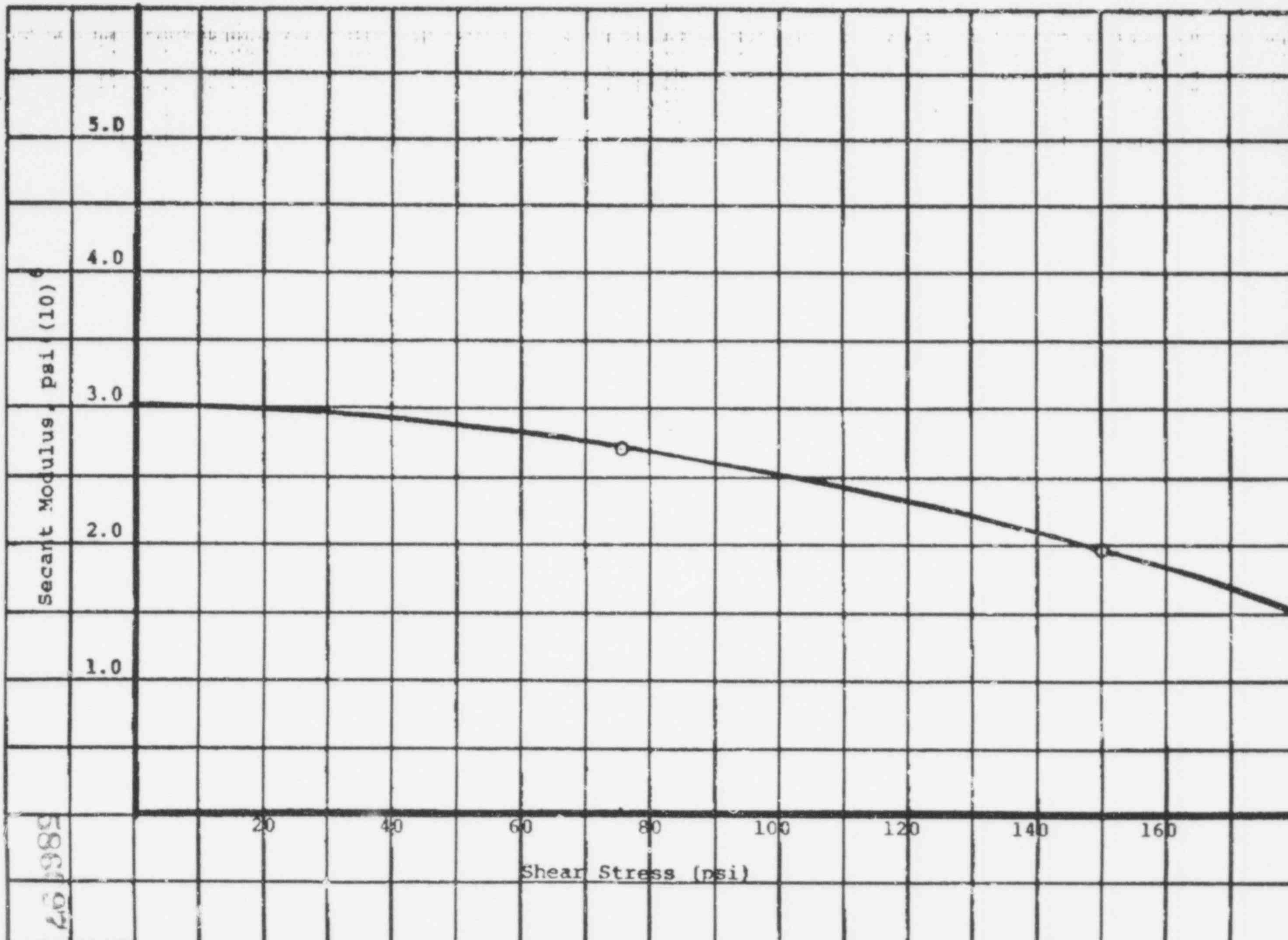

Figure 46- 20 Secant Modulus, Specimen L-2

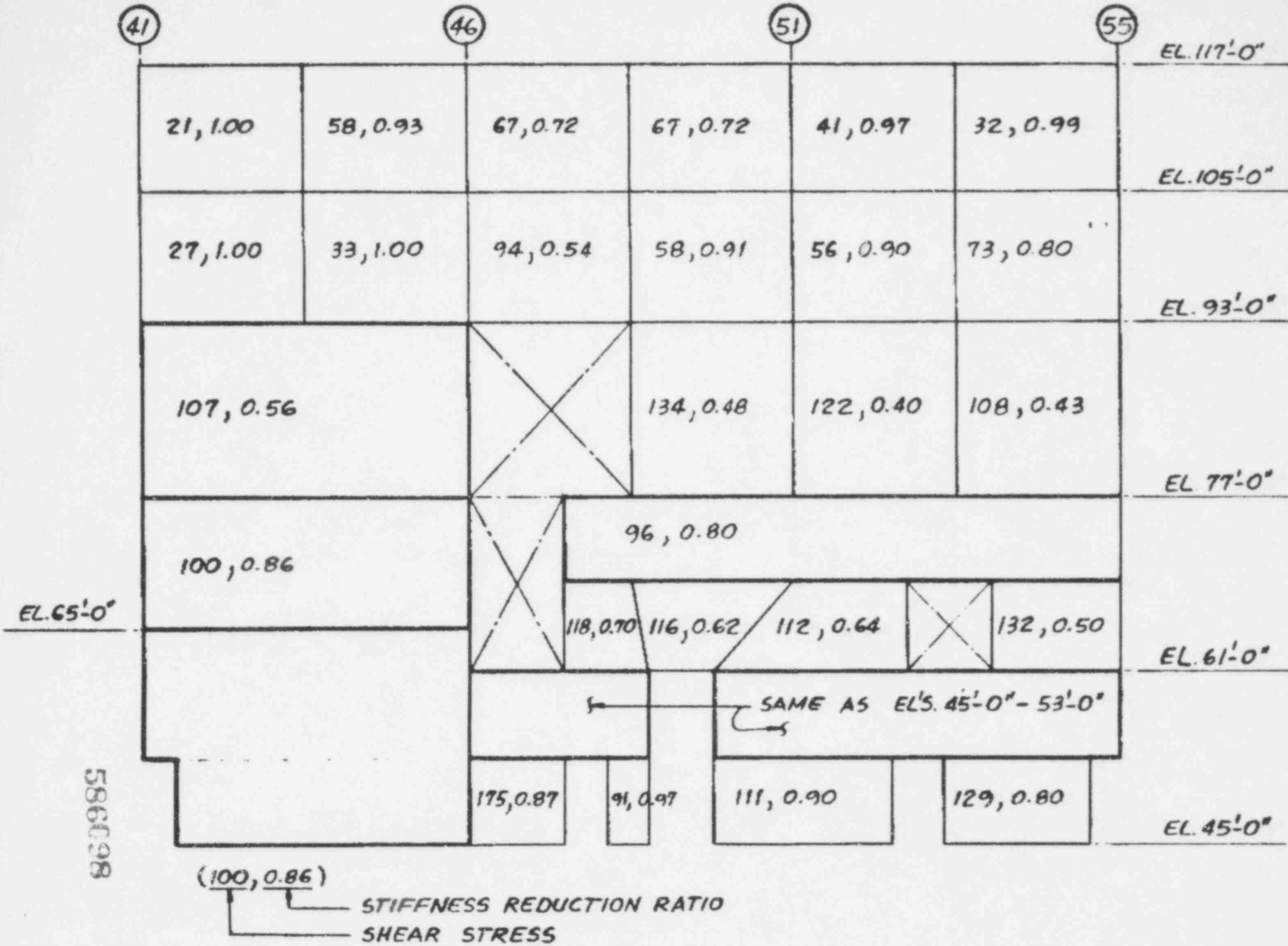

Figure 46-21 WALL (N) - CONTROL BUILDING

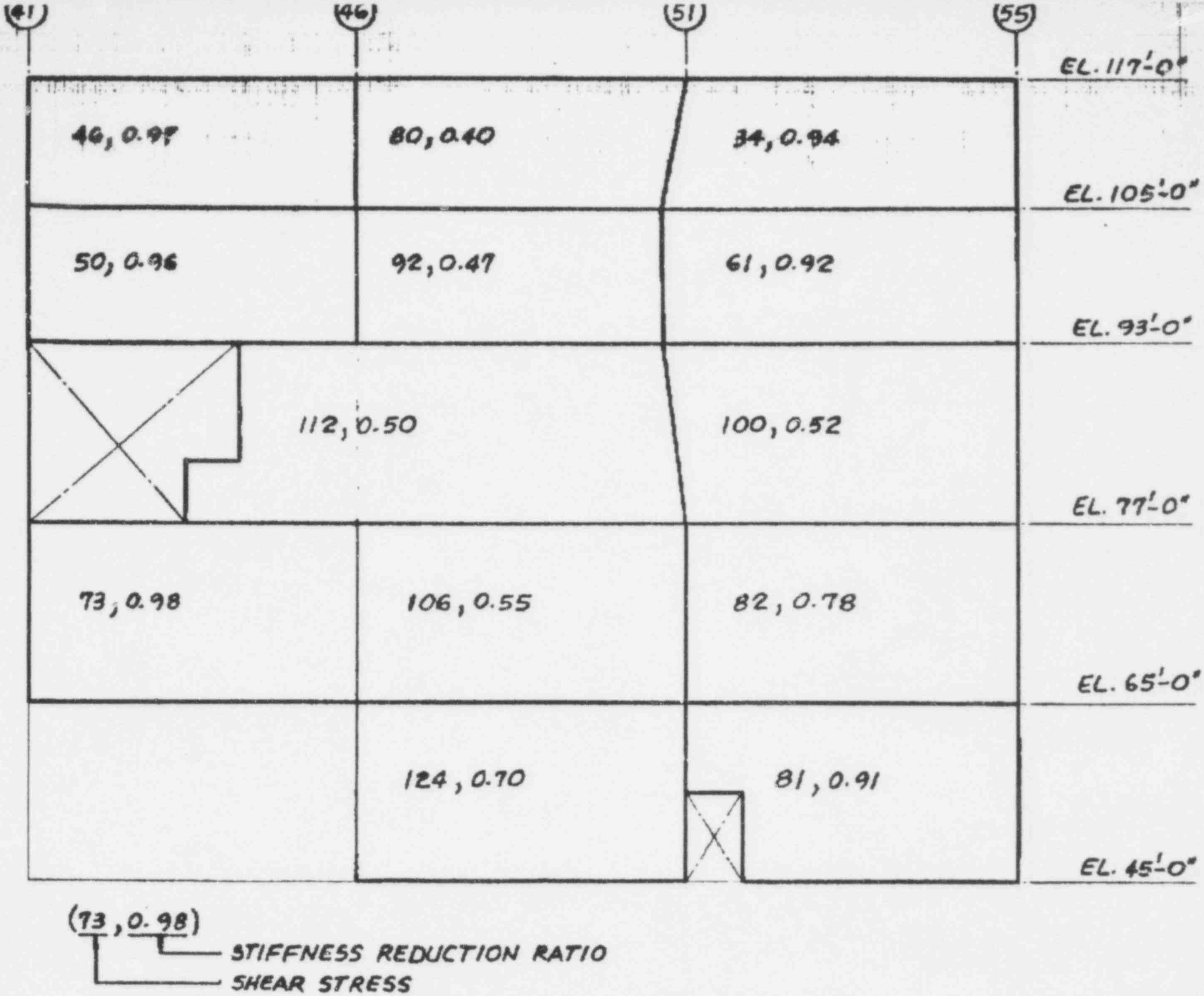

Figure 46-22 WALL (R) - CONTROL BUILDING

586099

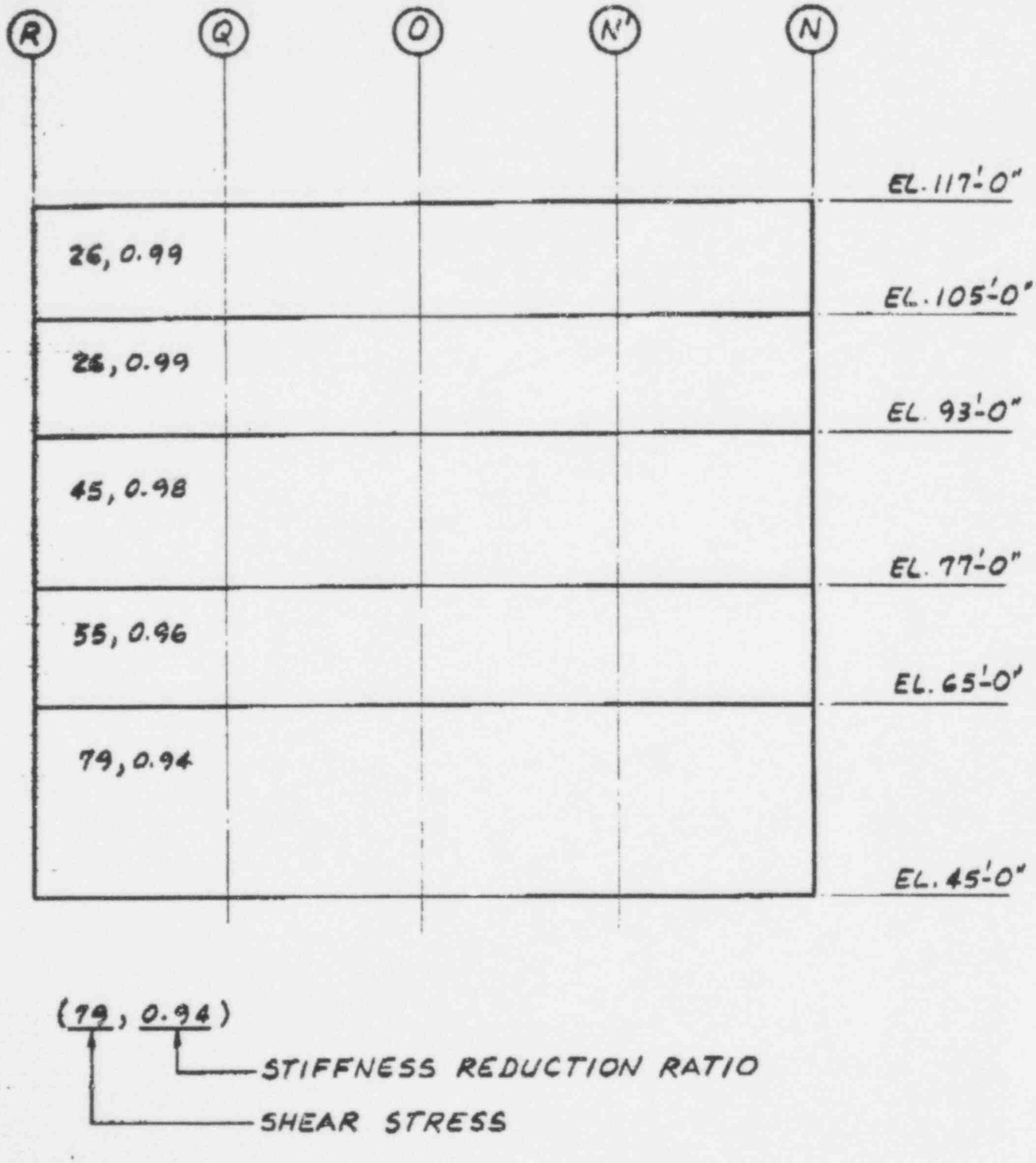

WALL (41) - CONTROL BUILDING

Figure 46-23

586100

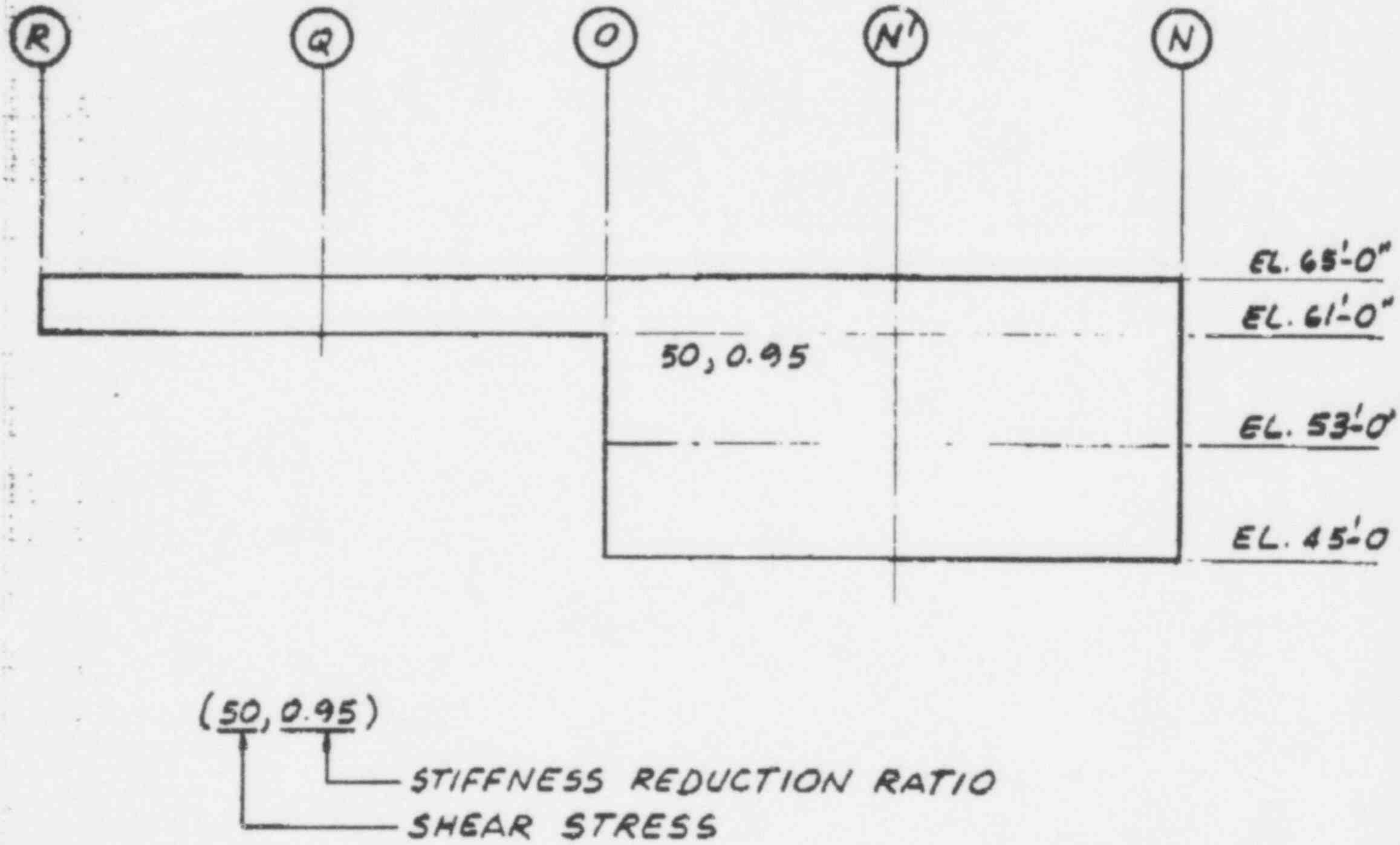

WALL 46 - CONTROL BUILDING

Figure 46-24

5861C1

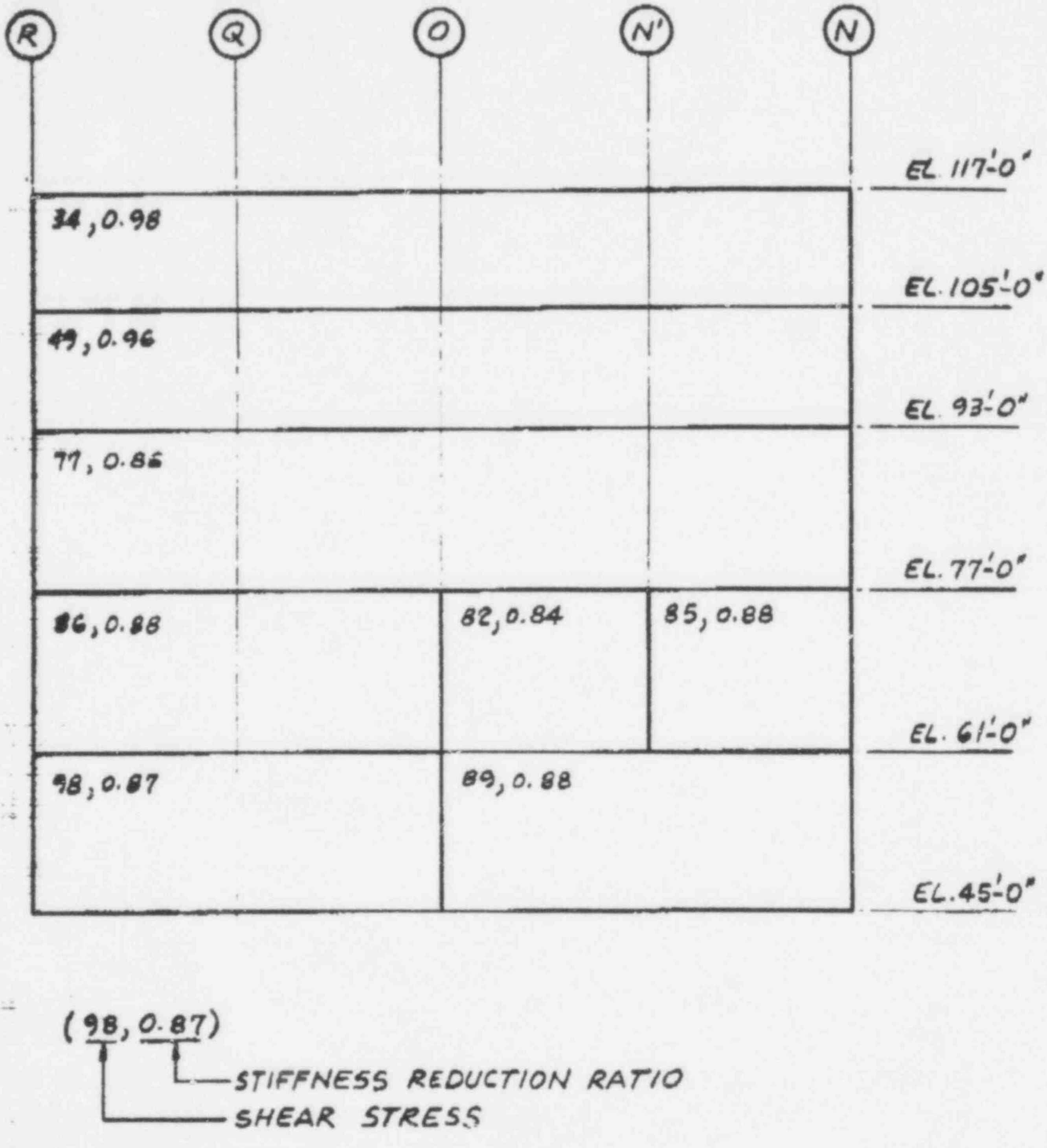

WALL 55 - CONTROL BUILDING

Figure 46-25

586102

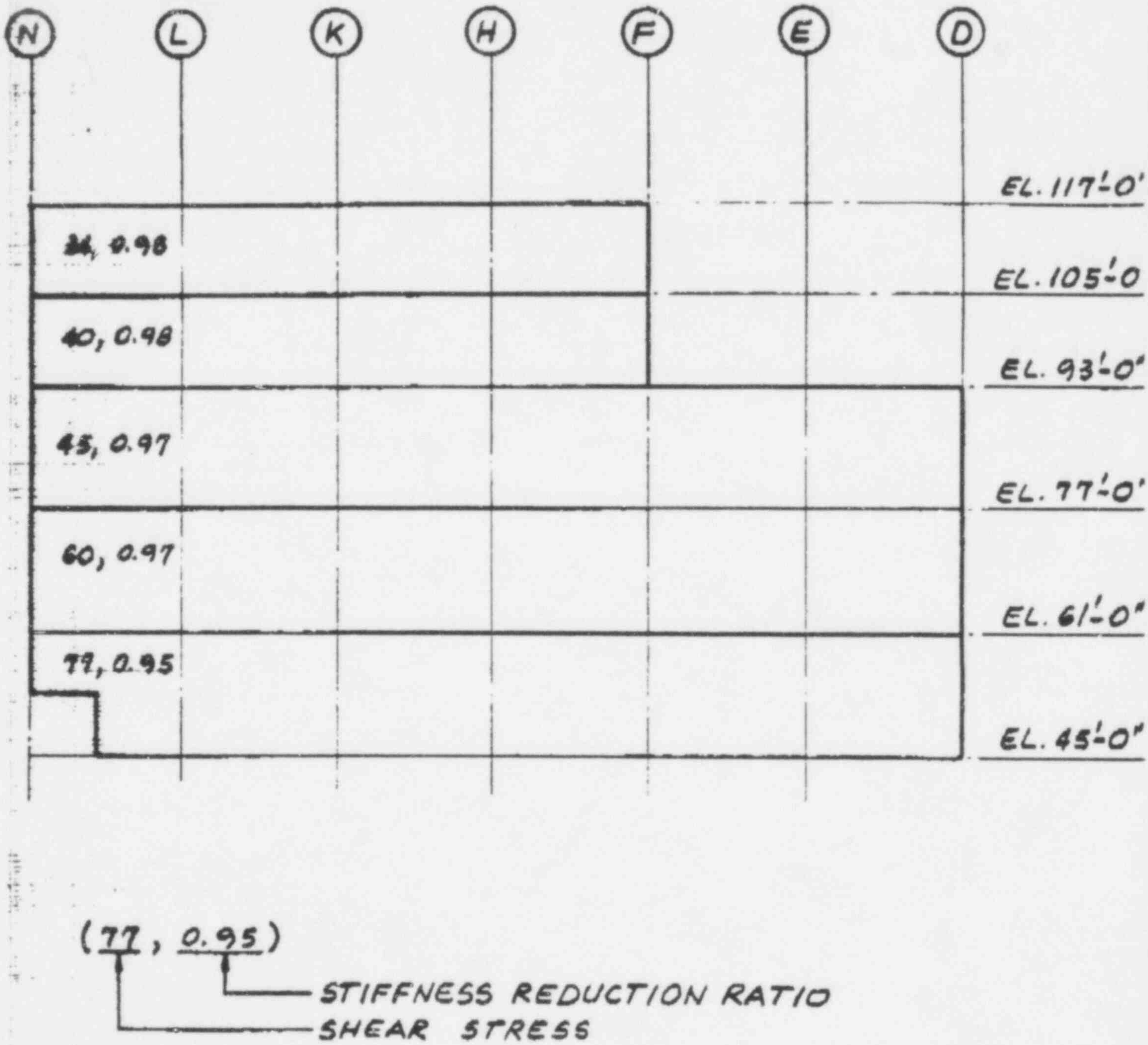

WALL (46) — AUXILIARY BUILDING

Figure 46-26

586103

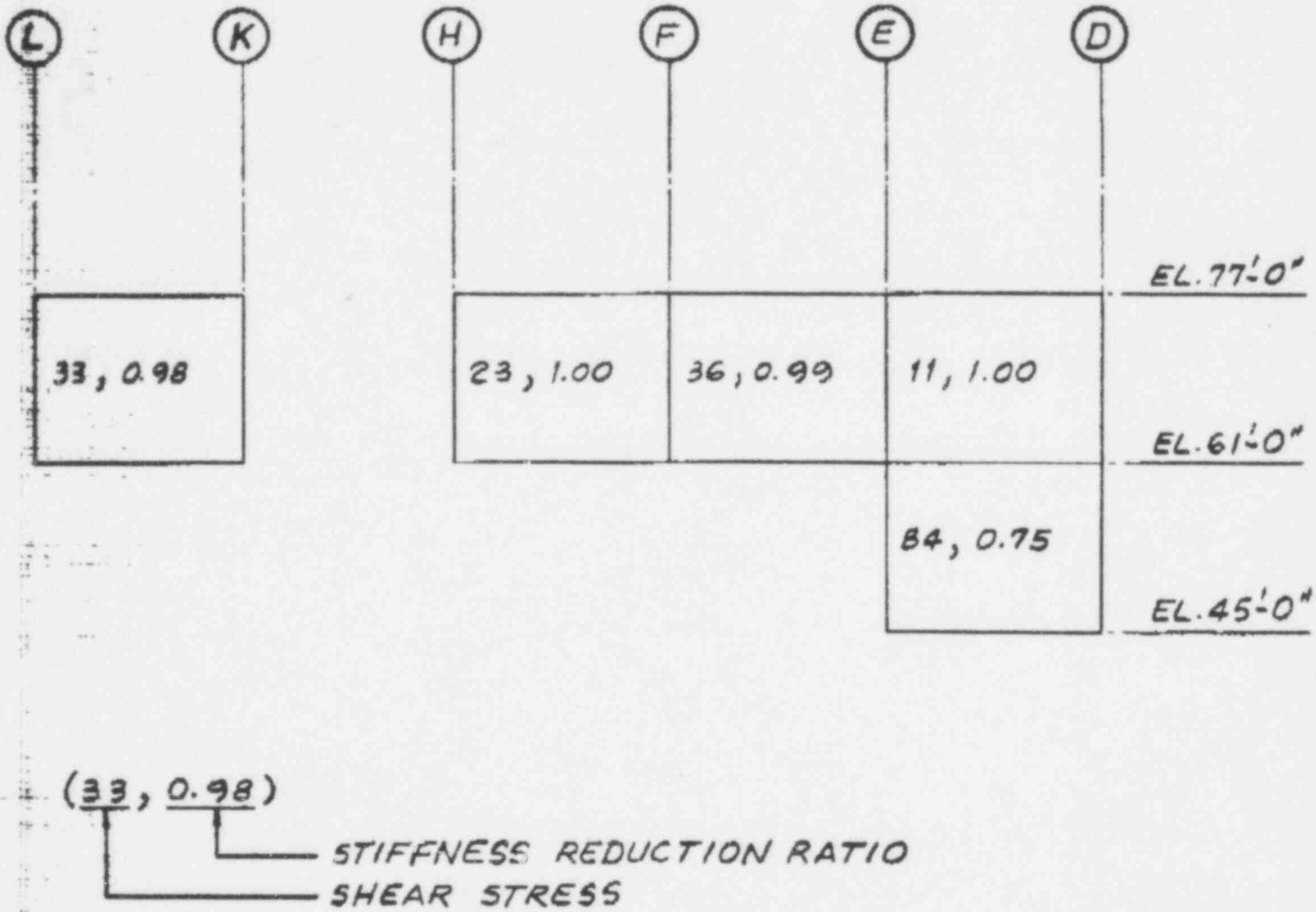

WALL 49 AUXILIARY BUILDING

Figure 46-27

586104

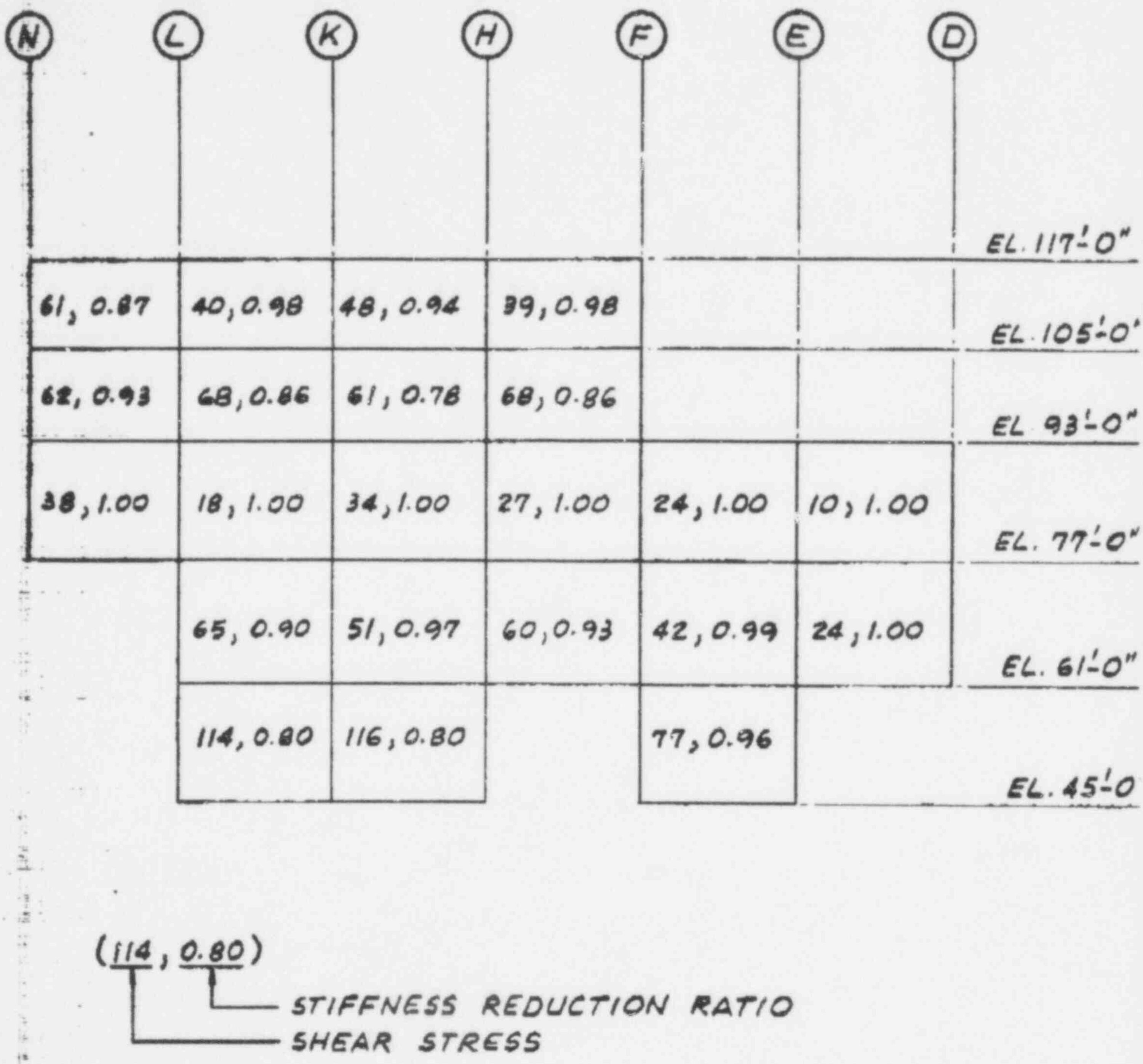

WALL 51 — AUXILIARY BUILDING

Figure 46-28

586105

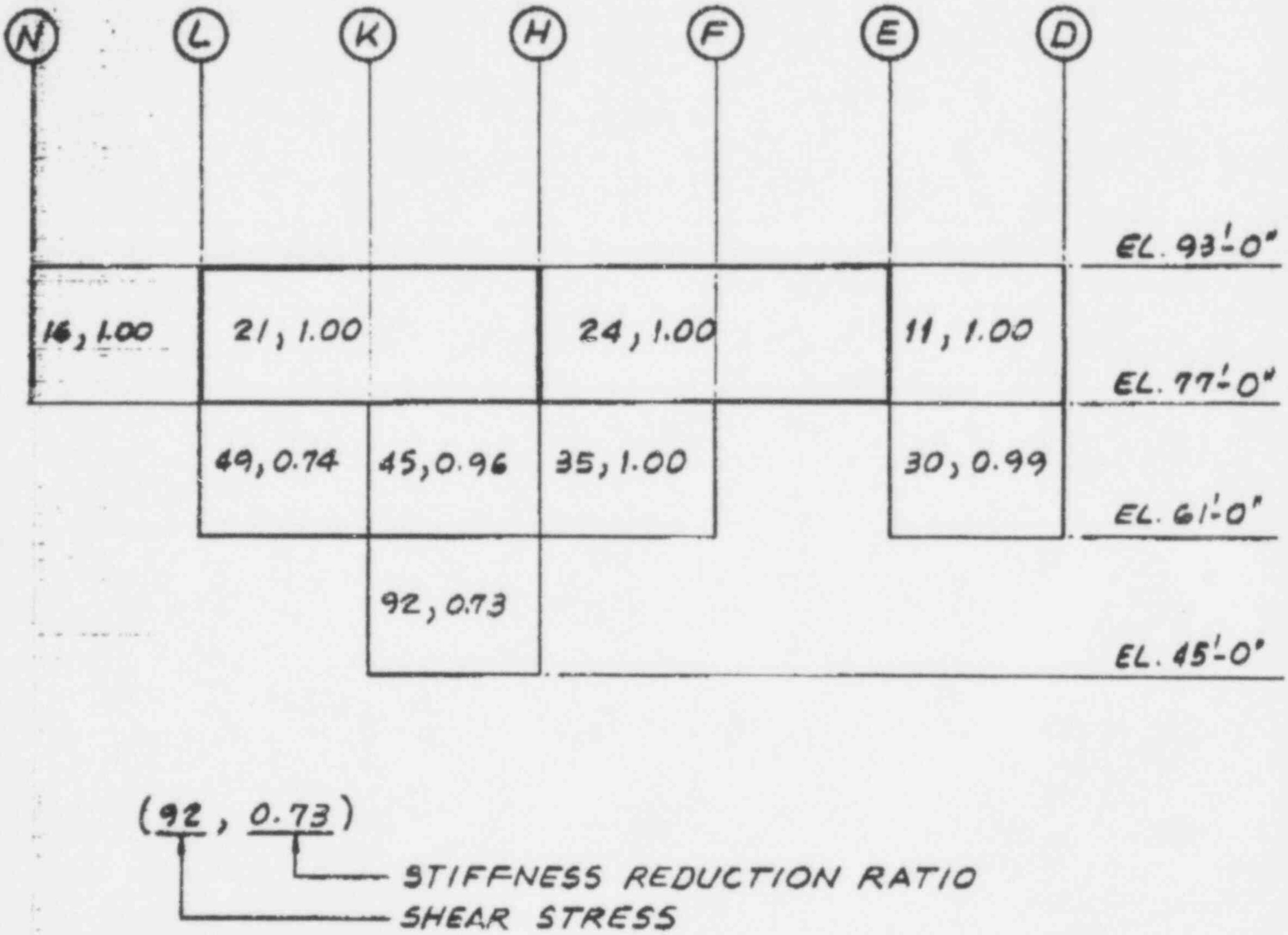

WALL 54 — AUXILIARY BUILDING

Figure 46-29

586106

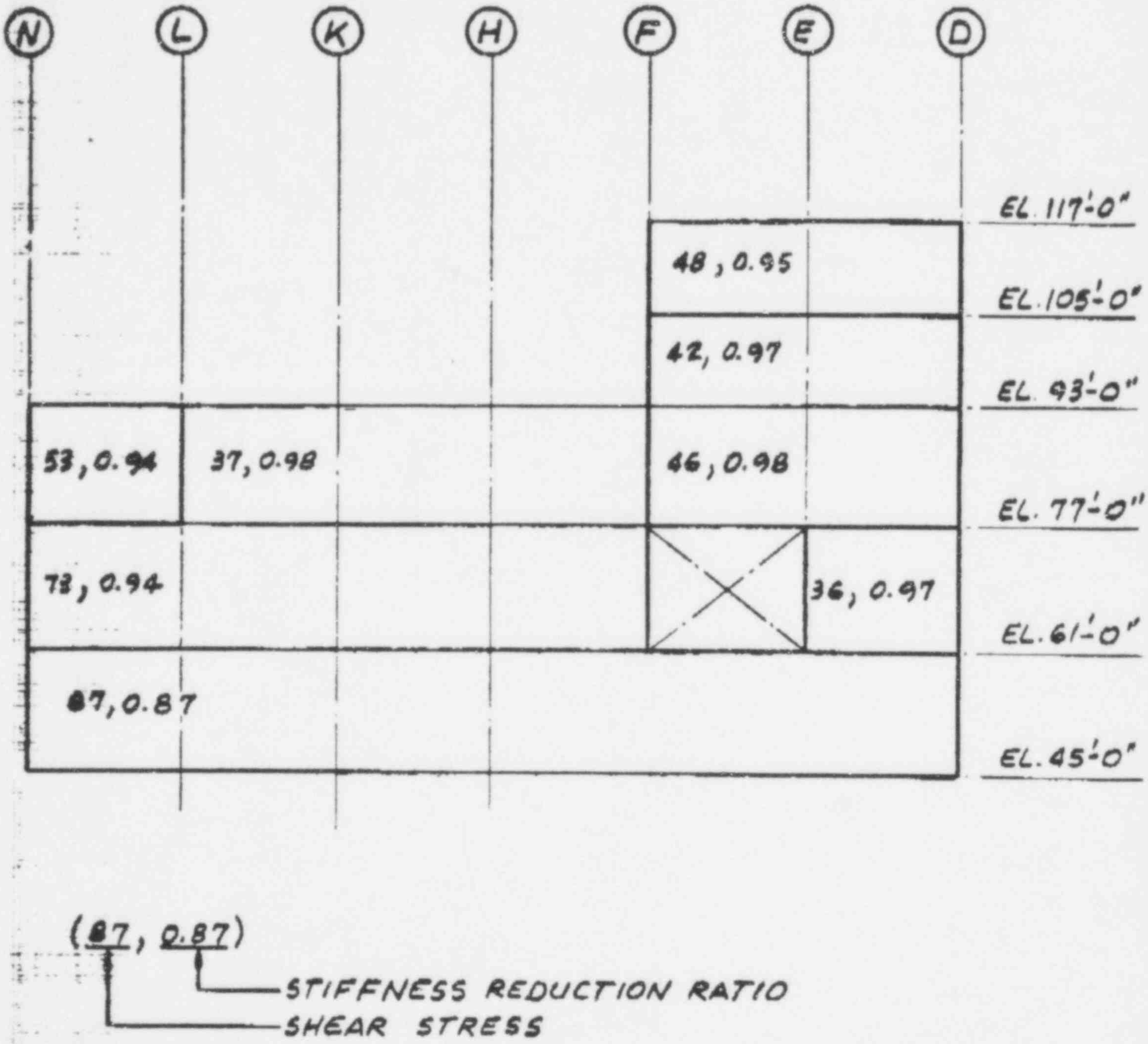

WALL 55 - AUXILIARY BUILDING

Figure 46-30

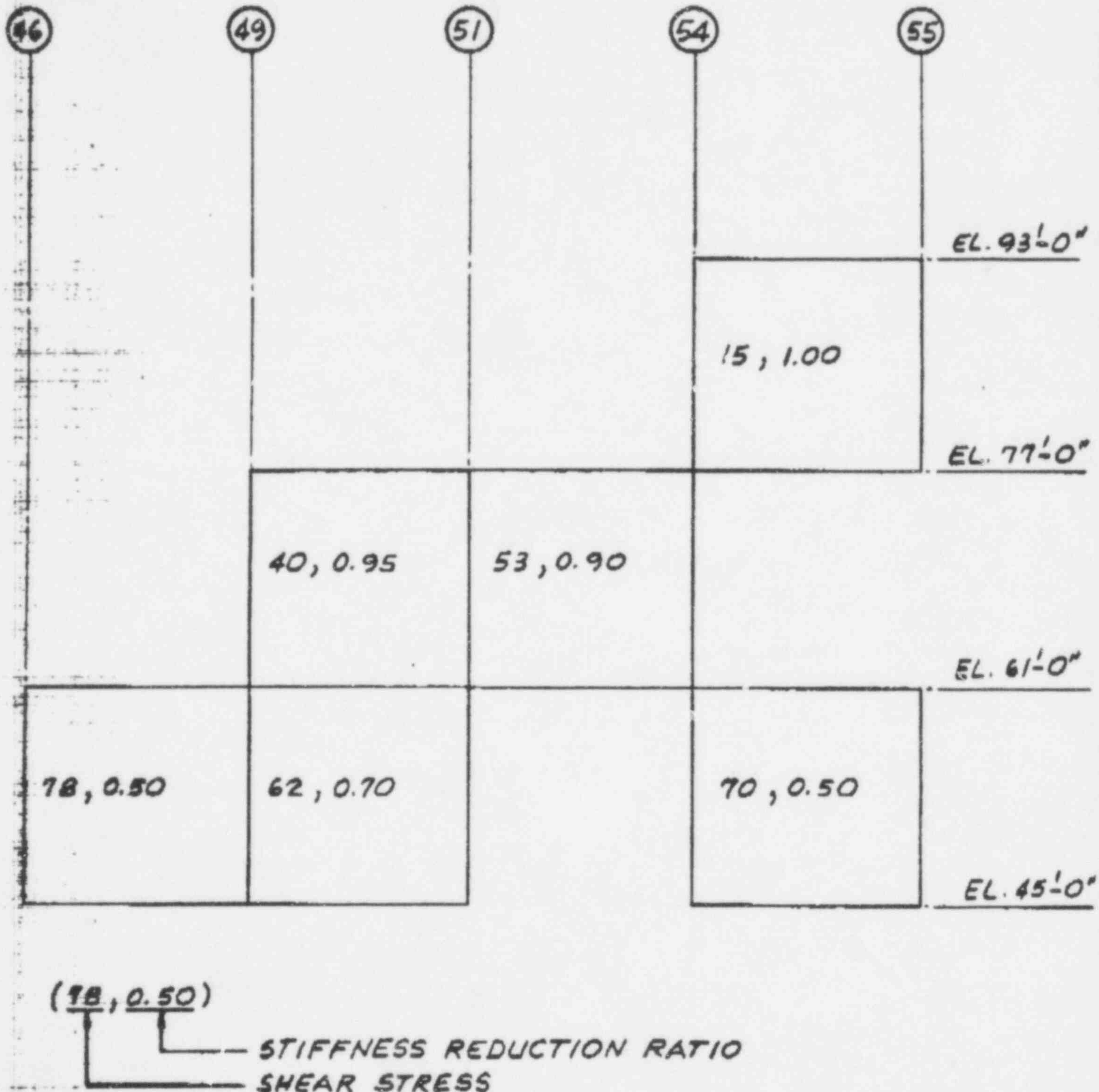

WALL (H) AUXILIARY BUILDING

Figure 46-31

5861(8

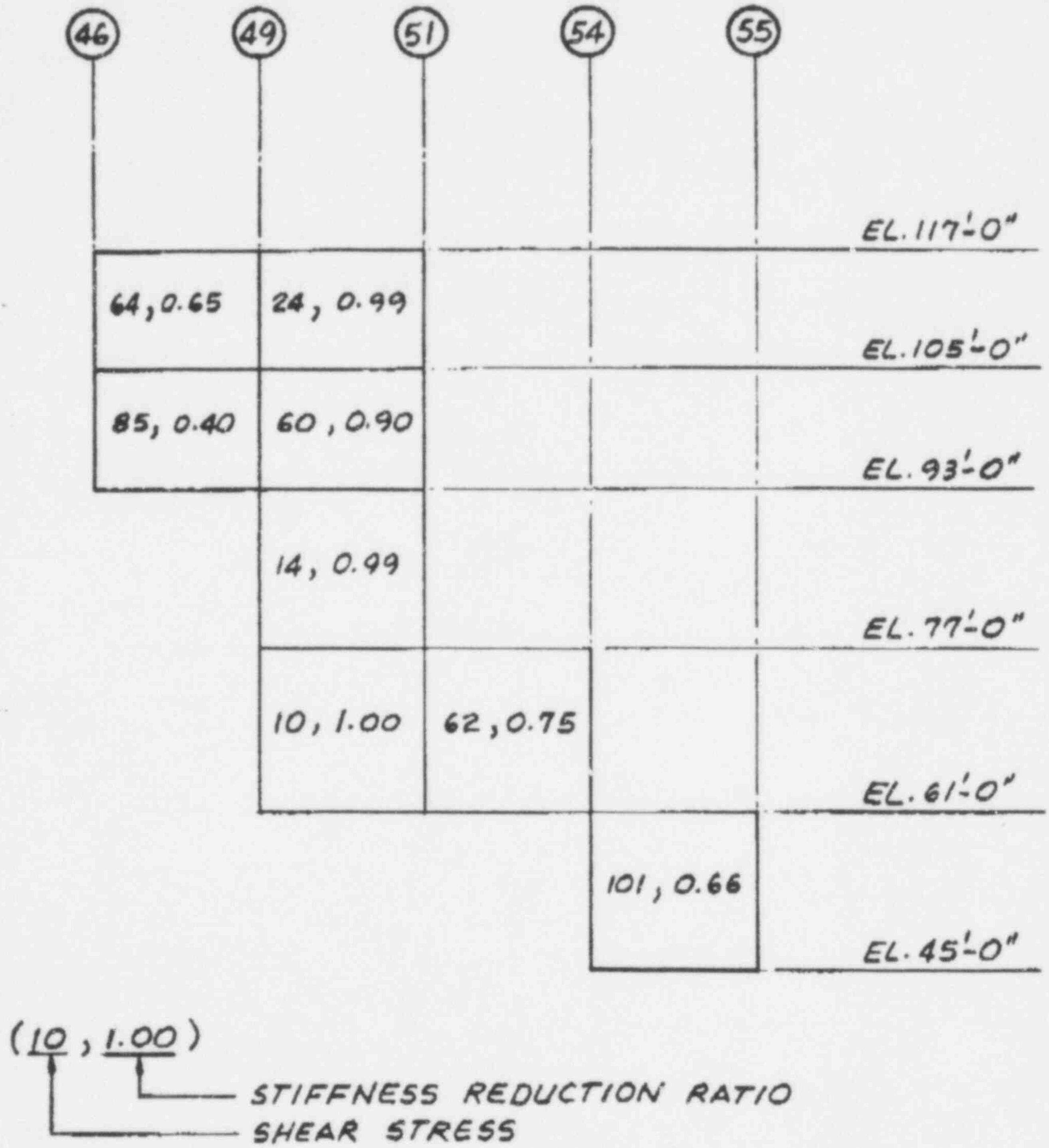

WALL AT LINE (K) AUXILIARY BUILDING

Figure 46-32

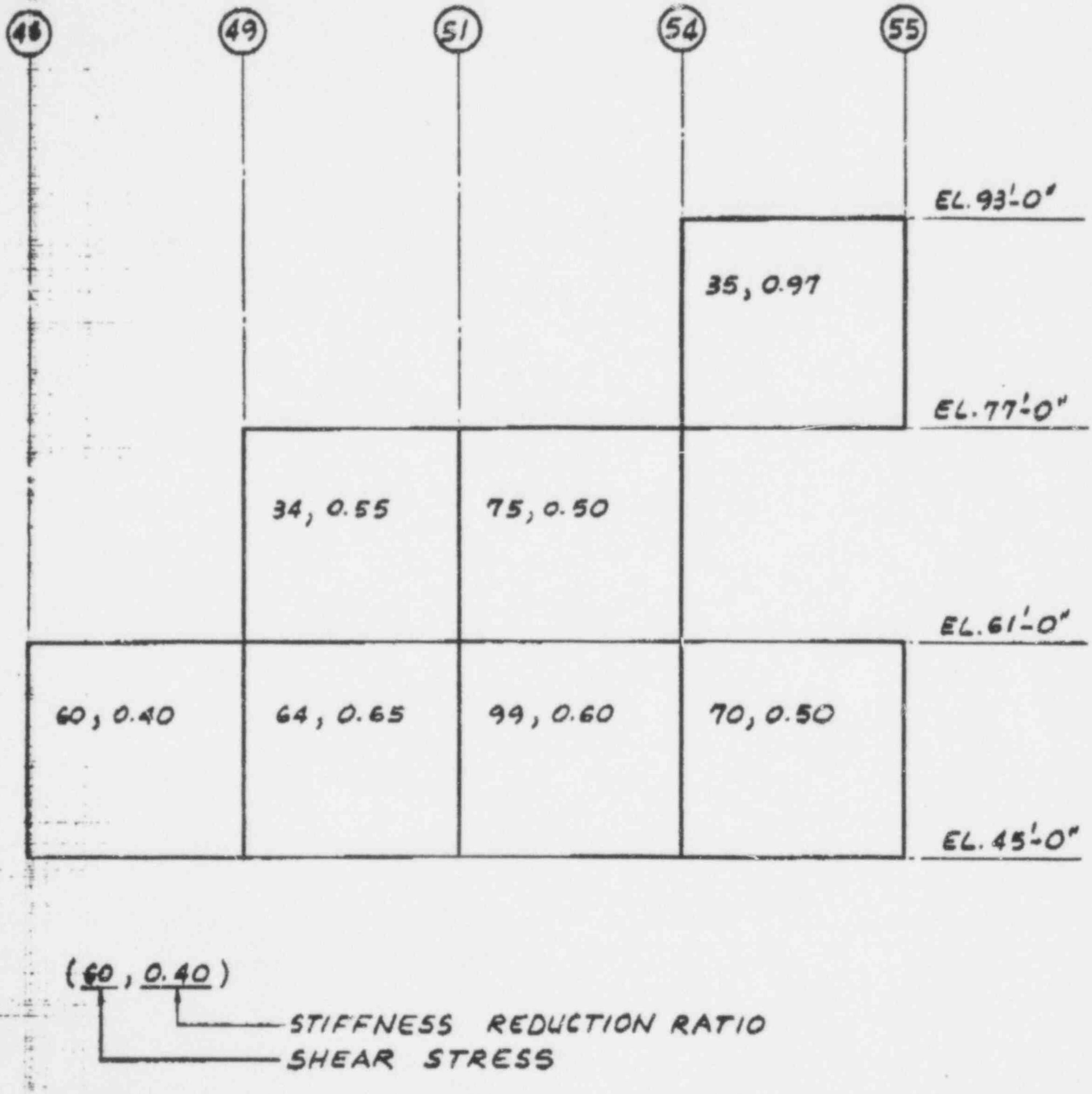

WALL (L) - AUXILIARY BUILDING

Figure 46-33

586110